

RESEARCH ARTICLE

Entry inhibition of HSV-1 and -2 protects mice from viral lethal challenge

Nicola Clementi^{a#}, Elena Criscuolo^a, Francesca Cappelletti^a, Paola Quaranta^b, Mauro Pistello^b,
Roberta A. Diotti^a, Giuseppe A. Sautto^{a*}, Alexander W. Tarr^c, Federico Mailland^d, Daniela Concas^e,
Roberto Burioni^{a,f}, Massimo Clementi^{a,f}, Nicasio Mancini^{a,f}

^aMicrobiology and Virology Unit, 'Vita-Salute San Raffaele' University, Milan, Italy

^bDepartment of Translational Research, University of Pisa, Pisa, Italy

^cSchool of Life Sciences & NIHR Biomedical Research Unit in Gastrointestinal & Liver Diseases,
Faculty of Medicine and Health Sciences, University of Nottingham, Nottingham, United Kingdom

^dScientific department, Polichem SA Lugano, Lugano, Switzerland

^eWezen Bio AG, Fondation pour Recherches Medicales, Geneva, Switzerland

^fLaboratory of Microbiology and Virology, San Raffaele Hospital, Milan, Italy

[#]Corresponding author. Nicola Clementi, Microbiology and Virology Unit, 'Vita-Salute San Raffaele'
University, 20132 Milan, Italy. E-mail address: clementi.nicola@hsr.it

*Present address: Giuseppe A. Sautto, Center for Vaccines and Immunology, Department of
Infectious Diseases, College of Veterinary Medicine, University of Georgia, Athens, GA, USA

N.C and E.C. contributed equally to this work.

Abstract

The present study focused on inhibition of HSV-1 and -2 replication and pathogenesis *in vitro* and *in vivo*, through the selective targeting of the envelope glycoprotein D. Firstly, a human monoclonal antibody (Hu-mAb#33) was identified that was able to neutralise both HSV-1 and -2 at nanomolar concentrations, including clinical isolates from patients affected by different clinical manifestations and featuring different susceptibility to acyclovir *in vitro*. Secondly, the potency of inhibition of both infection by cell-free viruses and cell-to-cell virus transmission was also assessed. Finally, mice receiving a single systemic injection of Hu-mAb#33 were protected from death and severe clinical manifestations following both ocular and vaginal HSV-1 and -2 lethal challenge. These results pave the way for further studies reassessing the importance of HSV entry as a novel target for therapeutic intervention and inhibition of cell-to-cell virus transmission.

Highlights:

- HSV-1 and -2 cross-protection is conferred *in vivo* by single post-infection systemic administration of a human anti-gD mAb
- This inhibitory activity of mAb results also in the inhibition of cell-to-cell virus transmission
- Fab#33, scFv#33 and IgG#33 engineered molecular formats of anti-gD mAb exert different anti-viral activity
- HSV-1 and -2 clinical isolates are more susceptible to mAb activity compared to reference virus laboratory strains

Keywords: HSV disseminated infection, cell-to-cell virus transmission, human antibodies, *in vivo* protection

1. Introduction

The global prevalence of HSV-2 is approximately 67%, lower than HSV-1. Nevertheless, HSV-2 still infects 19.2 million people every year with at least 3.4 million women infected in Africa (Looker et al., 2015). Thus, even a tiny proportion of severe HSV infections is a healthcare burden. Despite the availability of effective drugs, clinical isolates can be resistant to both first and second line drugs (acyclovir (ACV) and foscarnet (FOS), respectively) (Andrei and Snoeck, 2013; Schubert et al., 2014). The observed prevalence of ACV-resistant HSV in immunocompetent individuals is 0.1-0.6%, while FOS resistance has been found in about 60% of patients infected with these ACV-resistant viruses (Gilbert et al., 2002; Lascaux et al., 2012). All the available drugs exhibit nephrotoxicity when administered at high doses, thus limiting their clinical use in patients with impaired kidney function (Superti et al., 2008; Whitley and Roizman, 2001). Novel alternative or synergistic therapies are needed (Clementi et al., 2016), especially for the management of high risk patients such as new-borns, immunocompromised or post-transplant patients (Cherpes et al., 2012; Grinde, 2013; Whitley, 2006). Moreover, in immunocompromised patients the prevalence of ACV resistance increases to 4.3-14% (Gilbert et al., 2002). In this context inhibition of HSV entry may represent an additional therapeutic target. Among the classes of virus entry inhibitors the monoclonal antibodies (mAbs) are particularly versatile and have the advantage that their different engineered formats (single chain fragment variable (scFv), Fab fragment and whole-IgG) can meet both pharmacokinetic and pharmacodynamic needs while retaining their specificity for the target (Jefferis, 2012; Marasco and Sui, 2007), in addition, the use of human Abs generally reduces the risk of eliciting antidrug antibodies after administration in humans (Clementi et al., 2012; Presta, 2006). To date, several anti-HSV neutralising mAbs have been described (Berdugo et al., 2012; Burioni et al., 1994; Chen et al., 2004; Krawczyk et al., 2013; Lee et al., 2013; Nicola et al., 1998), but only a few are human-derived and inhibition of HSV infection by different

engineered antibody formats (Fab, scFv, IgG) has never been compared. In the present study, an anti-HSV Hu-mAb (mAb#33) was isolated and its different formats (Fab#33, scFv#33, IgG#33) were tested for their ability to inhibit virus infection both before and after virus entry (post-virus entry assays) using clinical isolates representing HSV-1 and HSV-2 with differing susceptibility to ACV. Finally, the mAb#33 format with the greatest potency *in vitro* was also tested *in vivo* using single systemic administrations against HSV-1 or -2 vaginal and ocular infections.

2. Materials and methods

2.1 Cells and Viruses

Vero E6 (Vero C1008, clone E6 - A TCC® CRL-1586TM) and HEK 293T (ATCC® CRL-1586TM) cells were both cultured in Dulbecco's Modified Eagle Medium (DMEM) containing 10% (v/v) fetal bovine serum (FBS). The laboratory strains HSV-1 HF (ATCC® VR-260™) and HSV-2 MS (ATCC® VR-540™) were used. Clinical isolates were kindly provided by Dr. R. Santangelo, Department of Microbiology, Università Cattolica del Sacro Cuore of Rome, Italy. The HSV-1 LV strain has been previously described (Tognon et al., 1985).

2.2 Mice

Female C57BL/6N mice, 8 weeks of age, were purchased from Charles River Laboratories (Sulzfeld, Germany) and housed and bred in a biosafety level 3 animal facility. Animals were maintained on 12/12-h dark/light cycle. Animal experiments were reviewed and approved by OPBA (Organismo Preposto al Benessere Animale) Università di Pisa and Ministero della Salute (Permit Number: n° 603/2015-PR) by the responsible authority DGSAF (Direzione Generale della Sanità Animale e dei Farmaci Veterinari), according to Italian Welfare Act (D.lgs. 26/2014. Art.31) and European regulations (2010/63/EU).

2.3 Generation and production of Fab#33

Fab#33 was selected using phage-display (Johnston et al., 2011; Solforosi et al., 2012). Briefly, a phagemid library was constructed from peripheral B cells of a donor showing strong serum IgG ELISA reactivity against both HSV-1 and -2 isolates. Fab#33 was selected against HSV-1 and -2 infected Vero E6 cells after deselection against uninfected cells, and subsequently affinity purified through a GammaBind Sepharose (GE Healthcare) column with goat anti-Human IgG Fab (ThermoFisher Scientific).

2.4 Other antibodies

The anti-HSV gD positive neutralisation control human Fab AC-8 (Burioni et al., 1994) was synthesised using its previously published amino acid sequence (Berdugo et al., 2012). Anti-HCV E2 e137 human mAb was used as negative experimental control (Perotti et al., 2008).

2.5 scFv#33 and IgG#33

scFv#33 was constructed using overlapping primers with the 15-amino acid (Gly₄Ser)₃ flexible hinge region respectively at 3' and 5', and purified following previously described protocols.

IgG#33 format was designed in our laboratory using the IgG1 constant region, and the large-scale production was performed by GenScript® using MamPower service. Briefly, target DNA were designed, synthesised and subcloned into pTT5 vectors for 293-6E cells co-transfection and expression. The cell supernatant was collected and affinity purified.

2.6 Neutralisation assays and post-entry inhibition assays

The biological activity of mAbs was determined *in vitro* using three different strategies.

2.6.1 Plaque assay

Serial concentrations of the different antibody formats were incubated with 100 plaque forming units (PFU) of virus (1 h at 37°C) in DMEM. Antibody-virus mixture was applied to Vero E6 monolayers. After 2 h, medium was replaced with complete DMEM with 2 % FBS and 1 % Agarose (BD) and plates were incubated for 46 h. Cells were then fixed and stained.

2.6.2 IN Cell Analyzer System analysis

Different antibody concentrations were incubated with 200 TCID₅₀ of virus for 1 h at 37 °C. Virus/antibody mixture was applied to Vero E6. After 2 h, medium was replaced with complete DMEM with 2 % FBS and plates were incubated for 21 h. Cells were fixed and stained with anti-HSV1+HSV2 gD murine antibody [2C10] (ab6507, Abcam) and Goat anti-Mouse IgG–FITC antibody (F0257, Sigma-Aldrich). Hoechst 33258 (Sigma-Aldrich) was used for nuclear staining. IN Cell Analyzer System allowed high-throughput acquisition and analysis was performed using IN Cell Investigator Software (Galluccio et al., 2014; Ranade et al., 2014).

2.6.3 Post-entry assay

The post-entry assay was adapted from Krawczyk et al., 2013 and De Logu et al., 1998 (De Logu et al., 1998; Krawczyk et al., 2013). Confluent monolayers of Vero E6 were infected with 100 PFU of virus. After 20 min of adsorption at 37°C, the virus was removed. Cells were then incubated for 46 h in DMEM containing 2 % FBS and 1 % Agarose in the presence of different mAb concentrations. Cells were fixed and stained. Images were acquired at 5-fold magnification. Viral plaques were counted and areas measured *in silico* using ImageJ 1.50c4 software (Rasband, ImageJ, U.S.N.I.H., Bethesda USA, <http://imagej.nih.gov/ij/>).

2.7 Cytofluorimetric binding assays

The binding activity of Fab#33 was assayed using HEK 293T cells transfected with glycoprotein D from HSV-1 HF (gD1) as described in the Supplementary Materials. After centrifugation cells were

fixed with 4 % paraformaldehyde and incubated for 30 min at room temperature with Fab#33 in presence or absence of the competitor anti-HSV gD AC-8 Fab (Burioni et al., 1994). Additionally, unrelated anti-HCV E2 e137 Fab (Perotti et al., 2008) was used as negative control as well as untransfected cells. The cells were then washed and incubated for 30 min at room temperature with goat anti-human IgG (H+L) Alexa Fluor® 488 (A-11013, ThermoFisher Scientific) or FITC-conjugated anti-FLAG [M2] (F4049, Sigma-Aldrich) antibodies. Afterwards, the cells were washed and analyzed by FACS. The FACS data were analyzed using FCS Express 6 Plus software (De Novo Software).

2.8 *In vivo* virus titration

In vivo titration via vaginal challenge of HSV-2 MS viral stock was performed in mice at 11 weeks of age, with their oestrous cycles synchronized (Teepe et al., 1990). Ten-fold dilutions of the viral stocks in DMEM (50 µL) were pipetted intravaginally under general anaesthesia. HSV-1 LV and HSV-2 MS viral stocks were used for *in vivo* titration via ocular challenge: under general anaesthesia, the right cornea was scarified and 5 µL of DMEM (2 % serum) containing 10-fold dilutions of the viral stocks was applied. The animals were then examined daily for apparent signs of infection. The lethal dose 50 (LD₅₀) of both viruses was assessed for each infection protocol (Fig. S10). The doses of both viruses for the different infection protocols were determined by observation of irreversible symptoms at day 8 post infection (p.i.) for HSV-2 MS (both for vaginal and ocular challenge) and at day 13 p.i. for HSV-1 LV. Mice that recovered from disease were followed up for 20 days p.i. and no relevant differences in their conditions, nor delayed onset of clinical symptoms were observed.

2.9 IgG#33 prophylactic and therapeutic activity against vaginal challenge

2.9.1 *In vivo* virus infections and treatments.

Eleven week old female mice were infected with 50 μL of HSV-2 MS (5×10^7 PFU) diluted in DMEM. Mice received 100 μL of IgG#33 (5 or 15mg/kg) diluted in PBS via lateral tail vein as a single dose 24 h before or 30 min after vaginal challenge. Anti-HCV IgG e137 (15mg/kg) was used as negative control. Groups consisted of 7 mice each, animals were sacrificed on day 8 to avoid unnecessary suffering. Animal experiments were approved by Pisa University and Ministry of Health, accordingly to national and European regulations (2010/63/EU).

2.9.2 Clinical disease scoring

Severity of genital lesions was scored as previously described (Chiuppesi et al., 2012). Animals were scored at baseline and at daily intervals. Clinical scores were reported starting from the onset of symptoms to the end of protocol (day 5 to 8).

2.9.3 Vaginal lavage viral titres

At 48 h post-challenge mice were anaesthetised, the vaginas were flushed with 50 μL of 1X PBS and the lavages stored at -80°C . Subsequently, 10 μL of vaginal lavage were applied to Vero E6 cell monolayers. After 2 h, inoculum was replaced with complete DMEM with 2% FBS and plates incubated for 21 h. Cells were fixed, stained and analysed using IN Cell Analyzer.

2.10 IgG#33 therapeutic activity against ocular challenge

2.10.1 *In vivo* virus infections and treatments

Under general anaesthesia, the right cornea was scarified (Berdugo et al., 2012). 5 μL of HSV-1 LV (5×10^4 PFU) or HSV-2 MS (5×10^5 PFU) diluted in DMEM was applied to scarified cornea. Eleven week old female mice received 100 μL of IgG#33 (15 mg/kg) i.v., or IgG e137 (15 mg/kg) as controls, diluted in 1X PBS via lateral tail vein as a single dose 30 min after infection. All groups

consisted of 5 mice each and all HSV-1 infected mice were sacrificed on day 13, while HSV-2 infected mice were sacrificed on day 8 to avoid unnecessary [suffering](#).

2.10.2 Clinical disease scoring

The severity of ocular disease was scored as previously described (Berdugo et al., 2012). Animals were scored at baseline and daily.

2.10.3 Tear film viral titres

At 2nd and 7th day p.i. mice were anesthetized and infected corneas were flushed [pipetting and recollecting 10 µL of DMEM containing 2 % serum](#) (Berdugo et al., 2012). [The tear film content was added to 190 µL of medium](#), stored at -80 °C and analysed as for vaginal lavages. Moreover, 10 µL of tear film samples were used for viral DNA extraction (QIAGEN) and genomic copies quantified using ELITeMGB[®] Kit (ELITechGroup) for Real-Time PCR analysis.

2.10.4 Tissue preparation and Immunohistochemistry

Kidneys and eyes from each group were dissected, fixed and mounted in Killik (Bio-Optica) at -80 °C for cryosectioning. Frozen cryosections were rinsed, incubated in 0.1% Triton X-100, blocked with 1% BSA (Sigma-Aldrich), and incubated overnight at 4°C with anti-HSV1+HSV2 gD antibody [\[2C10\] \(ab6507, Abcam\)](#). Samples were incubated for 1 h at 20 °C with Goat anti-Mouse IgG (H+L) Alexa Fluor 546[®] ([A-11030, ThermoFisher Scientific](#)) and Alexa Fluor 488[®] Phalloidin ([A12379, ThermoFisher Scientific](#)). Hoechst was used for nuclear staining. Slides were observed at 63- and 10-fold magnification.

2.11 Statistical analysis

All data analyses and statistics were performed using GraphPad PRISM[®] (GraphPad Software, San Diego California USA, www.graphpad.com). One-way ANOVA was performed for repeated

measures followed by Bonferroni post-test was performed for the evaluation of plaque area inhibitory activity of the different [Hu-mAb#33](#) engineered formats. The same test was performed for the comparison of reduction of plaque number of the different mAb engineered formats in post-entry assays. Kaplan-Meier survival curves were compared using the log-rank (Mantel-Cox) test considering p value 0.05 as threshold for statistical significance. Two-way ANOVA with Bonferroni post-tests were used to perform statistical comparisons between the different mean disease clinical scores observed for each treated mouse cohort. [One-way ANOVA followed by Kruskal-Wallis test was used for statistical analysis of data generated by titres of vaginal lavages. T-test followed by Welch's correction was used for statistical analysis of data generated by titres and genomic copies quantification assays of tear film samples.](#)

See Supplementary for fully detailed Material and Methods

3. Results

Prior to choosing the antibody format to be evaluated in animal infection models, the [Hu-mAb#33](#) was produced in three different molecular formats: Fab, scFv and IgG. After the identification of the virus glycoprotein recognised by [Hu-mAb#33](#), all the three formats were first tested for their ability to neutralise viruses belonging to both HSV-1 and 2, including clinical isolates with different susceptibility to ACV in *in vitro* phenotypic assays. Their inhibitory activity was tested in a newly developed post-entry assay performed at 37 °C, allowing virus entry into target cells to test the ability of [scFv#33](#), [Fab#33](#) and [IgG#33](#) to inhibit virus replication and even more importantly, cell-to-cell transmission, when added after virus infection in semi-solid culture medium. Based on the lower IC₅₀ and potent post-entry inhibitory activity compared to other molecular formats, [Hu-](#)

mAb#33 IgG was chosen for testing *in vivo* its capability to protect mice from lethal virus vaginal and ocular HSV-1 and -2 virus challenge.

3.1 Generation of an anti-HSV-1 and HSV-2 cross-reactive Hu-mAb and target identification

A Hu-mAb was generated as Fab fragment (**Fab#33**) using optimised biopanning procedures from peripheral B-lymphocytes of a donor showing strong serum IgG reactivity in ELISA against HSV-1 and -2 isolates (**Fig. S1**). **Fab#33** selectively recognised HSV-1 HF- and HSV-2 MS-infected cells (**Fig. S2A**). Western-blotting (WB) analysis on purified HSV-1 particles (**Fig. S3A**) and indirect immunofluorescence (IIF) analysis on cells transfected with HSV-1 HF gD or HSV-1 HF gB (**Fig. S3B**) were also performed. Both assays demonstrated the specific binding of **Fab#33** only on gD-transfected cells.

3.2 Evaluation of anti-HSV neutralising activity

Fab#33 neutralising activity was assessed by plaque reduction assays (PRA) against both HSV-1 and -2. **Fab#33** The IC₅₀ values against HSV-1 HF and HSV-2 MS were calculated to be 0.76µg/mL and 0.118µg/mL, respectively. **Fab#33** potency was also determine by micro-neutralisation assay followed by automated IIF counting, with IC₅₀ values of 0.612 µg/mL for HSV-1 HF and 0.135 µg/mL for HSV-2 MS (**Fig. S4, S5, Table 1**). Both assays confirmed that **Fab#33** neutralises both HSV types at low nanomolar concentrations: 2.7nM (HSV-2 MS) and 12.24nM (HSV-1 HF).

3.3 Evaluation of post-entry inhibitory activity

The ability of **Fab#33** to inhibit replication of HSV-1 and -2 even after infection was evaluated using a specifically adapted PRA in which the **Fab#33** was dissolved in low concentration DMEM-agar medium. Both number and area of plaques were quantified. **Fab#33** reduced the number of HSV-1 HF plaques by 18.92 % and HSV-2 MS plaques by 57 % at 50 and 200 µg/mL (Krawczyk et al., 2013) (**Fig. 1A**). **Fab#33** reduced the mean plaque area by 43.5 %, even at 100 µg/mL on HSV-2

MS-infected cells, whereas no significant reduction in plaque area was observed on HSV-1 HF-infected cells ($p>0.05$) (Fig. 1B). Fab#33 post-entry activity was also compared with that of anti-HSV Hu-Fab AC-8, already described for its neutralising activity against both HSV-1 and -2 (Berdugo et al., 2012; Burioni et al., 1994; De Logu et al., 1998) (Fig. 1A, B). No significant differences between the two Fabs were observed in reduction of plaque number for HSV-2 MS infection ($p>0.05$), while only Fab#33 slightly decreased the number of plaques on HSV-1 HF infected cells ($p<0.05$). No differences were observed in plaque area reduction for HSV-1 HF. Interestingly, Fab#33 exhibited greater potency than AC-8 against HSV-2 MS (43.5% reduction by 100 μ g/mL Fab#33, vs 24.3% reduction by 200 μ g/mL AC-8) (Fig. 1A, B). A competition assay between the two Fabs was also performed by FACS analysis of cells transfected with gD1. Some competition, decreasing in a dose-dependent manner, was observed at higher AC-8 concentration (10 μ g/mL) using Fab#33 at low concentration (1.5 μ g/mL) for all the tested AC-8 concentrations (Fig. 1C).

3.4 Evaluation of *in vitro* activity of different engineered Hu-mAb#33 formats: scFv#33, Fab#33 and IgG#33

To evaluate the biological activity of different antibody formats, scFv#33, Fab#33 and IgG#33 formats were produced and tested for their ability to bind, neutralise and inhibit HSV post-entry replication. Both IgG#33 and scFv#33 bound to cells infected with HSV-1 HF or HSV-2 MS isolates (Fig. S2B) Comparison of their neutralising activity revealed that IgG#33 possessed IC₅₀s of 1.092 μ g/mL (HSV-1 HF) and 0.731 μ g/mL (HSV-2 MS) (Table 1, Fig. S5). No appreciable neutralising activity was observed for scFv#33.

	IC ₅₀ µg/mL (nM)		
	ScFv#33	Fab#33	IgG#33
HSV-1 HF	>10 (400)	0.612 (12.24)	1.092 (7.28)
HSV-2 MS	>10 (400)	0.135 (2.7)	0.731 (2.44)

Table 1. Neutralising activity of different Hu-mAb#33 engineered formats.

scFv#33 and IgG#33 inhibition of HSV infection was then assessed using the adapted PRA (Fig. 2A, B and S7A, B and S8A, B). In this case, scFv#33 in semi-solid medium inhibited the number of infectious events by 29.6 % on HSV-2 MS infected cells at 200 µg/mL and by 24.2 % at 50 µg/mL. scFv#33 inhibited the number of infection HSV-1 events by 22.16 % at 50 µg/mL. In contrast, IgG#33 strongly inhibited HSV-2 MS infection events in a dose-dependent manner spanning from 93 % inhibition at 100 µg/mL, to 40 % inhibitory activity at the lowest tested concentration (6 µg/mL). No significant inhibition of viral events (6.57 %) was observed for IgG#33 format against HSV-1 HF at the highest concentration (25 µg/mL). Both scFv#33 and IgG#33 formats potently reduced HSV-2 MS plaque areas in a dose-dependent manner. scFv#33 inhibited virus spreading by 99.8 % at 200 µg/mL and plaque area was inhibited by 90 % at 100 µg/mL and by 63.2 % at 12.5 µg/mL. IgG#33 almost completely eliminated plaque area (98.2 % reduction) of HSV-2 MS at 100 µg/mL and by 44.2 % at 6 µg/mL. scFv and IgG formats inhibited HSV-1 HF virus cell-to-cell spread by 91.7 % at 50 µg/mL and 94.2 % at 25 µg/mL respectively.

3.5 Evaluation of IgG#33 anti-HSV activity against HSV-1 and 2 clinical isolates

The cross-protection conferred by IgG#33 was evaluated against different clinical isolates from patients with different clinical manifestations: #1 (oral lesions), #8 (pharyngeal swab), #7 (bronchoalveolar lavage), #11 (labial vesicles), #LV (neurotropic strain (Tognon et al., 1985)) for HSV-1, and #18 (cutaneous lesions), #21 (vaginal discharge) #25 (vaginal lesions), #26 (cutaneous lesions) and #28 (cutaneous lesions) for HSV-2. All the isolates featured different susceptibility to

ACV (**Fig. S9**). As depicted by **Table 2** and **Fig. S6**, **IgG#33** was able to potently neutralise all tested clinical isolates at very low IC₅₀.

HSV-1	IgG#33 IC ₅₀ µg/mL (nM)	HSV-2	IgG#33 IC ₅₀ µg/mL (nM)
HF	1.092 (7.28)	MS	0.731 (2.44)
#1	0.306 (2.04)	#18	0.696 (4.64)
#7	0.741 (4.94)	#21	0.519 (3.46)
#8	0.632 (4.21)	#25	0.379 (2.53)
#11	0.558 (3.72)	#26	0.463 (3.09)
LV	0.436 (2.91)	#28	0.656 (4.37)

Table 2. Neutralising activity of IgG#33 vs HSV clinical isolates featuring different susceptibility to ACV in vitro.

IgG#33 post-entry activity was evaluated against LV and #26 virus isolates (**Fig. 3A, B**). **IgG#33** inhibited the number of plaques of HSV-1 LV by 76.85 % at 25µg/mL ($p<0.05$), and by 45.68 % at 3 µg/mL ($p<0.05$). **IgG#33** showed even greater activity against HSV-2 #26, showing 94.18 % inhibition at 100 µg/mL and 52.13 % inhibition at 10 µg/mL ($p<0.05$). **IgG#33** reduced plaque areas by 98 % at 100 µg/mL on HSV-2 #26 and by 75.3 % at 25 µg/mL on HSV-1 LV.

3.6 Prophylactic and therapeutic activity of **IgG#33** against vaginal HSV-2 challenge

A single systemic injection of **IgG#33** (5 mg/Kg or 15 mg/Kg) *via* lateral tail vein was performed 24 h prior or 30 min post HSV-2 MS infection (30 minutes are sufficient for virus entry (Vahlne et al., 1980)). Kaplan-Meier survival curves (**Fig. 4A**) revealed that both **IgG#33** dosages conferred 100 % protection from death (7/7 mice survived) 8 days p.i., compared to control groups in both settings (5/7 mice died; 71.43% mortality) ($p=0.0075$). No statistical difference at day 8 p.i. ($p=0.1356$) was observed between negative control IgG treated mice (2/7 mice died) and infection control (5/7 mice died) in prophylactic protocol, while in a therapeutic setting 6/7 mice died in the unrelated

IgG mock control group ($p=0.0019$). The mean clinical disease scores revealed that both IgG#33 single doses strongly inhibited clinical manifestation of HSV-2 infection compared to infection and mock controls (**Fig. 4B**). Clinical scores were reported from the onset of symptoms to the end of protocol (day 5 to 8). Mean clinical disease scores of prophylactic protocol were: 1.571 to 2.857 for HSV-2 infection control group; 0.643 to 2.114 for the group receiving unrelated IgG; 0.143 to 0.286 for IgG#33 5 mg/Kg; and 0 to 0.571 for the group receiving 15 mg/Kg IgG#33. Mean clinical disease scores of therapeutic protocols were: 1.571 to 2.857 for HSV-2 infection control group; 1.357 to 3.643 for the group receiving unrelated IgG; 0.143 to 0.286 for the group receiving 5 mg/Kg IgG#33 and 0.143 to 0.357 for the group receiving 15 mg/Kg IgG#33. Both IgG#33 concentrations significantly reduced mean disease score compared to virus infection control starting from day 6 p.i. ($p<0.05$) as well as to the group receiving the unrelated IgG ($p<0.01$). Mice treated with IgG#33 in both experimental settings did not present clinically relevant manifestations of HSV-2 infection, whereas symptoms in control animals spanned from erythema and ulcers to nervous system involvement (**Fig. 4C**). Finally, vaginal lavages collected 48 h p.i. from the different mouse cohorts were tested for their infectious viral load using cell-based infection assays (**Fig. 4D**). A significant reduction in viral load was observed in lavages collected from IgG#33-treated groups compared to untreated groups ($p<0.01$). Titres (FFU/mL) detected in vaginal lavages of prophylactic protocol mice were: 7.7×10^5 in the virus infection control group, 1.2×10^5 in the IgG#33 (5 mg/Kg)-treated group, 6.4×10^4 in the IgG#33 (15 mg/Kg) group and 6.4×10^5 in the unrelated IgG group. For therapeutic protocol groups were: 7.7×10^5 in the virus infection control group, 2.7×10^4 in the IgG#33 (5mg/Kg) group, 1.9×10^4 in the IgG#33 (15mg/Kg) group and 2.2×10^5 in the unrelated IgG (15mg/Kg) treated group . p values are reported in **Fig. 4**.

3.7 Therapeutic activity of IgG#33 against HSV-1 and HSV-2 ocular challenge

A single systemic administration of **IgG#33** (15mg/Kg) was performed 30 min after HSV-1 LV (neurotropic strain) or HSV-2 MS ocular infections, fully protecting mice from death (**Fig. 5A**). All HSV-1 infected mice were sacrificed on day 13, while HSV-2 infected mice were sacrificed on day 8, to avoid unnecessary suffering. Specifically, **IgG#33** conferred 100% protection (7/7 mice alive) at 13 days p.i. against HSV-1 LV in contrast to 71.43% mortality rate (5/7 mice died) observed for control groups ($p=0.007$). **IgG#33** fully protected mice (7/7 alive) against HSV-2 MS compared to controls ($p=0.022$ vs virus infection control, and $p=0.007$ vs unrelated IgG). No differences were observed between virus control and an unrelated IgG groups ($p=0.590$). Mean clinical disease scores (Berdugo et al., 2012) were evaluated between days 1-8 p.i. (**Fig. 5B**). For HSV-1 LV protocol, mean of symptom scores were evaluated between days 1-13 p.i.: 0 to 3.714 for virus control group; 0 to 4.571 for unrelated IgG and 0 to 0.143 for **IgG#33**-treated mice, indicating almost complete protection conferred by **IgG#33** from ocular HSV-1 infection compared to controls ($p<0.001$ from day 8). Mean clinical scoring of HSV-2 MS infections were: 0 to 3.929 for the virus control group; 0 to 4.643 for unrelated IgG, and 0.071 to 0.214 for **IgG#33**-treated mice. Mice receiving **IgG#33** were significantly protected from HSV-related severe disease compared to controls. Mice receiving **IgG#33** occasionally developed milder symptoms after HSV-infection but they completely recovered from them. In contrast, control mice developed severe movement impairment indicating neural involvement and severe HSV ocular symptoms (**Fig. 5C**). Virus titres and quantification of HSV genome copies on tear films collected on days 2 and 7 p.i. were also evaluated (**Fig. 5D**): titres (FFU/mL) in tear samples of mice challenged with HSV-1 and receiving **IgG#33** were 1.2×10^4 at day 2, and 7.9×10^2 at day 7; 4.3×10^4 infected cells at day 2 and 1.4×10^4 at day 7 were observed for the unrelated IgG tear samples. In mice infected with HSV-2 titres (FFU/mL) were: 5.4×10^3 at day 2 and 1.1×10^2 at day 7 for **IgG#33** cohort, and 1.2×10^4 at day 2 and 1.5×10^3 at day 7 for mice receiving control IgG. The same samples were also tested for the

presence of HSV genomes. The median number of genome copies for mice challenged with HSV-1 were: 272.4 Nc(gEq/ μ L) at day 2 and 0 Nc(gEq/ μ L) at day 7 for mice receiving IgG#33; 1783 Nc(gEq/ μ L) at day 2 and 17.71 Nc(gEq/ μ L) at day 7 for mice receiving unrelated IgG. The median number of genome copies for mice challenged with HSV-2 were: 3241 Nc(gEq/ μ L) at day 2 and 0 Nc(gEq/ μ L) at day 7 for mice treated with IgG#33; 733.2 Nc(gEq/ μ L) at day 2 and 182.9 Nc(gEq/ μ L) at day 7 for unrelated IgG controls. Only IgG#33-treated mice completely cleared viral DNA and infectious viral load in tear films within 7 days for both HSV challenges. Of note, the viral load was nearly undetectable in lavages of IgG#33-treated mice at day 7 p.i.. p values are reported in Fig. 5.

3.8 Histological analyses

Four kidney anatomical compartments (capsule, cortex, medulla, pelvis) of mice treated with IgG#33 or unrelated IgG control after HSV ocular infections were analysed (Fig. 6A). Mice receiving systemic IgG#33 presented normal tissue architecture for all the anatomic compartments, while mice receiving unrelated IgG control possessed altered tissue architecture, especially for medulla and pelvis. With the exception of the capsule, tissues dissected from control mice were found to possess virus. Eyes dissected from IgG#33-treated mice and unrelated IgG control group were analysed, but no morphological differences were detectable. However, higher virus prevalence was detected in all compartments belonging to HSV-1 control cohort (Fig. 6C) compared to mice treated with IgG#33 (Fig. 6B), in which virus was restricted to its entry route (cornea) leaving the retina almost virus-free. Unfortunately, eye cryosections of mice challenged with HSV-2 MS were not properly compared due to virus tissue damage (Fig. S11).

4. Discussion

We investigated, both *in vitro* and *in vivo*, the anti-viral activity of an anti-gD human monoclonal antibody, mAb#33. The mAb was engineered in three different antibody formats (scFv, Fab, IgG) to compare both neutralising activity and ability to inhibit cell-to-cell transmission of both HSV type 1 and 2. This informed the choice of the best candidate to be administered in mice receiving lethal HSV challenge.

The neutralising activity of the Fab fragment was evaluated against HSV for the first time, by micro-neutralisation assay coupled with InCell Analyzer automated count, allowing fine evaluation of Fab IC₅₀ due the ability to test more experimental conditions and more replicates in the same experimental session, reducing experimental variability. Results from this assay were also confirmed by standard PRA. To the best of our knowledge the IC₅₀ calculated for Fab#33 against HSV-1 and -2 are amongst the lowest described so far for Fabs of human origin. It is important to highlight, however, that potent neutralising activity does not always translate to good *in vivo* efficacy (De Logu et al., 1998; Dimmock, 1993). In the case of HSV a low IC₅₀, while indicative of function, is not the only anti-viral effect to be evaluated. It is well known that HSV infects cells both as cell-free virus and *via* cell-to-cell transmission mechanism. The latter can be barely affected even by a neutralising antibody since the virus passes through cell junctions without release from infected cells. As such we evaluated the inhibitory activity of Fab#33 even when added to cells after virus infection performed at 37°C in semi-solid medium, minimising the infection events due to cell free virus. To do this we adapted the post-virus entry assay described by Krawczyk et al., 2013 and De Logu et al., 1998 (De Logu et al., 1998; Krawczyk et al., 2013) to assess the inhibitory activity of the tested molecules the cell-to-cell transmission. In these experiments we also included as a control the human anti-gD Fab better characterised for its biological activity so far, the AC-8 (Berdugo et al., 2012; Burioni et al., 1994; De Logu et al., 1998; Sanna et al., 1996; 1999; 2000; Zeitlin et al., 1996). The post-entry assays revealed greater activity

of the Fab in reducing both number and area of plaques for HSV-2 MS compared to that observed against the HSV-1 HF laboratory strain, where only the number of plaques was slightly reduced, and in sharp contrast, no reduction in plaque area occurred. The broad activity of Fab#33 against HSV-1 HF and HSV-2 MS might be due to the differences in terms of amino acid substitutions between the two virus laboratory strains (**Fig. S13**), potentially impairing Fab affinity. This is also consistent with the higher Fab#33 IC₅₀ against HSV-1 HF compared to that against HSV-2 MS. These observations for Fab#33 are similar to that of the control mAb AC-8 against the same virus isolates, the only exception being the total lack of plaque number reduction by AC-8 Fab against HSV-1 HF strain. Additionally, the overall similar behaviour of Fab#33 and AC-8 in post-entry assays is also consistent with the reported IC₅₀ of AC-8 against HSV-2, lower than those described against HSV-1. This is supported by the competition observed in FACS analyses performed between the two Fabs. As briefly introduced above, the Fab#33 was also engineered in other two antibody formats: the scFv and the whole IgG1 tested for both neutralising activity and inhibition of virus replication after virus entry. Unexpectedly, despite IgG#33 potentially neutralising both HSV-1 and -2, including clinical isolates featuring reduced susceptibility to acyclovir, the scFv format did not show any neutralising activity at the highest concentration tested (IC₅₀>10µg/mL). The same scFv potentially reduced plaque area for both HSV-1 and -2 but had limited impact on plaque number. Accordingly, IgG#33 potentially inhibits plaque area for both virus types, consistent with its potent inhibition of HSV-2 plaque number but discordant with its weak inhibition of HSV-1 plaque number. As observed above for Fab format, the different activity in post-entry assays might be due again to differences between amino acidic gD sequences of HSV-1 HF and -2 MS affecting the IgG binding affinity. The post-entry activity of the three antibody formats was then compared to their post-virus attachment activity using previously-described procedures (Burioni et al., 1994). In this case virus adsorption was performed at 4 °C, allowing the docking of virus anti-receptors with

cell receptors but impairing cell entry until the switch to 37 °C performed after the 4 °C addition of antibodies. Inhibition was observed for all tested antibody formats (Fig. S12), with no significant differences between the different formats for HSV-2 MS. Conversely, both IgG and scFv demonstrated better HSV-1 HF inhibition compared to the Fab#33. It is noteworthy that the assay performed at 4 °C resulted in inhibitory activity by the scFv format against both virus types, in contrast to the standard neutralisation assays. The exact processes underlying the mechanisms involved in mAb#33-mediated inhibition remain to be determined, but the inhibitory activity in post-entry assays of mAb#33 (especially scFv and IgG formats) was robust and reproducible. A possible explanation for the observed effect might be the different steric hindrance of IgG compared to the Fab format. Notwithstanding this, this is in over contrast with the behaviour of the scFv format in the same assay, which although lacking any neutralising activity featured a strong plaque area decreasing activity. An explanation of this paradoxical activity might be found in the possible mAb#33 interference of gD-mediated triggering of gB fusogenic activity. As suggested by the complete lack of neutralising activity by the scFv#33 it is probably directed against gD regions not directly involved in binding to cellular receptors. The observed neutralising activity of the Fab and the whole IgG formats may therefore only be an effect of increasing steric hindrance, inhibiting binding to the target cell. This specific feature was not directly addressed in the present paper but, in our opinion, certainly deserves further investigation, as far as mAb#33 epitope definition is concerned. Two potential mechanisms have been described for the triggering of fusion by gD in its post-docking conformation. In one setting, gD exposes its PFD thus triggering gB already bound to its receptors (Cohen et al., 1986; Gallagher et al., 2014; 2013; Stampfer et al., 2010). In the other, gD binds to its receptors causing displacement of the gD C-terminus to expose a previously hidden region, which then interacts to gH/gL dimer, leading to its activation. The dimer activated form subsequently interacts with gB regulating fusion process (Atanasiu et al.,

2013; Gianni et al., 2015; Jackson et al., 2010). Although both mechanisms could be supported by the different functional behaviour of the three engineered formats of Hu-mAb#33, further dedicated studies are certainly needed to define its mechanisms of action and its epitope.

Overall, the *in vitro* results and the interference with different phases of HSV spread suggested a potential application of mAb#33 in different HSV-related clinical manifestations. Given the higher *in vitro* efficacy against both HSV-1 and -2 laboratory strains of IgG#33 compared to its Fab and scFv antibody formats, we then tested its activity against different HSV-1 and -2 clinical isolates. IgG#33 possessed potent neutralising activity against these clinical isolates and, surprisingly, resulted in an even stronger post-entry reduction of plaque number and greater inhibition of plaque area against the tested isolates. Importantly, we observed that HSV-1 isolates, including the LV neurotropic isolate (Tognon et al., 1985), are more susceptible to IgG#33 than the previously tested lab strain HSV-HF. It is important to note that the viruses tested were isolated from different replication sites from patients affected by different HSV-1 and -2 clinical manifestations and featured different susceptibility to ACV. These findings pave the way to the possible use of IgG#33 to treat diverse clinical HSV manifestations that are not susceptible to ACV treatment. Importantly, the IgG#33 target is completely different and unrelated to that of ACV, highlighting the potential for therapeutic co-administration with “classical” drugs for the treatment of patients suffering for drug nephrotoxicity. Given the promising *in vitro* results, *in vivo* testing of IgG#33 was a logical progression of these studies. However, several mAbs able to neutralise HSV have been described so far. Most them are directed against viral gD or gB are murine (Däumer et al., 2011; Lazear et al., 2012; Minson et al., 1986; Muggeridge et al., 1990; Nicola et al., 1998), fewer are of human origin (Burioni et al., 1994; Lee et al., 2013). We decided to develop a human antibody to both minimise the risks of anti-IgG response and avoid Ab-humanisation processes necessary for therapeutic mAb administration. It is well known that

repeatedly administering mAbs in humans may induce anti-idiotypic and anti-allotypic antibodies. However, these adverse effects were documented mostly when administering animal-derived antibodies, whereas humanised mAbs were well tolerated. These side-effects do not occur for human monoclonal antibody administrations (De Logu et al., 1998; Knox et al., 1991). In the case of HSV the most protective and best characterised human/humanised mAbs recognise virus gD or gB of both HSV-1 and -2 (Berdugo et al., 2012; Krawczyk et al., 2013; 2015; Lee et al., 2013; Sanna et al., 1996; Zeitlin et al., 1996; 1998). Among the most promising anti-gD mAbs are E317 and AC-8. The structural basis for recognition of gD antigen by the neutralising E317 Fab have been elucidated through co-crystallisation approaches. AC-8 is the only human anti-gD mAb tested on animals in different experimental settings. Topical administration of AC-8 in different antibody formats (Fab, F(ab')₂, IgG1) was tested by Zeitlin et al. (Zeitlin et al., 1996) concomitantly to HSV-2 vaginal challenge, demonstrating for the first time the potential of topical passive immunisation with a human anti-gD mAb to both prevent lesions and reducing virus shedding. Another important advance was testing topical administration of AC-8 Fab against HSV-1 KOS corneal infection (Berdugo et al., 2012). The Fab was able to significantly limit disease and reduce virus titres within tear films, but was not as effective as trifluridine (TFT). Non-topical administration of anti-gD human IgG AC-8 protected SCID mice from both intra-cutaneous and ocular HSV-1 challenge (Sanna et al., 1995). IgG AC-8 was administered intraperitoneally prior to, or after virus infection significantly prolonging mice survival. To date, intravenous systemic administration of human anti-gD antibodies has not been described. However, HSV generally causes viremia followed by severe sequelae only in circumscribed clinical settings such as immunocompromised patients or new-borns, therefore, an interesting option was to test intravenous single administration of IgG#33 before or after HSV-1 and -2 ocular and vaginal lethal challenge. In both prophylactic and therapeutic HSV-2 intravaginal infection experiments IgG#33 was injected at two

doses (5 and 15 mg/Kg) compatible with possible clinical use (Glassman and Balthasar, 2014). Both IgG doses fully protected mice from death in both experimental protocols. The main difference observed between these experiments was the greater reduction in virus titre in vaginal lavages from mice therapeutically treated with IgG#33, and the milder clinical signs compared to both control cohorts. However, in the prophylactic protocol the unrelated IgG partially protected mice from death at the end of experiments (8 days p.i.). Despite this, all the mice treated with the unrelated mAb control experienced greater disease progression in contrast with those treated with IgG#33, consistent with an increased virus titre (statistically significant only in the prophylactic experiment) measured in vaginal lavages of mice receiving the control IgG. An explanation for this partial protection from death but not from relevant clinical signs could be the immunogenic boost conferred to C57BL/6 immunocompetent mice by the systemic administration of mAbs before the virus challenge. A single systemic IgG#33 administration through lateral tail vein protected also mice challenged with both HSV types *via* corneal scraping. The protection against HSV-1 ocular challenge conferred by systemic mAb administration is consistent with previous studies using an anti-gB humanised antibody (Krawczyk et al., 2015). IgG#33 protected mice from both death and severe HSV clinical manifestations over all experimental durations. Moreover, all mice receiving IgG#33 that presented milder disease completely recovered during the follow-up period. In this experimental setup, the follow-up was 13 days p.i. for HSV-1 challenged mice and 8 days p.i. for those infected with HSV-2. Due to the severe and very rapid development of irreversible clinical manifestations observed for mice not receiving IgG#33, the HSV-2 challenged mice were sacrificed according to ethical committee directives. Consistent with clinical scoring data, the analysis of viral infectious load in tear films collected from the different mice treated cohorts established that all mice receiving IgG#33 almost completely cleared both infective virions and HSV-1 and -2 genome copies. Virus clearance at day 7 p.i. was completely

independent of both the number of HSV genome copies detected and of viral titre of samples collected at day 2 p.i.. These assumptions are consistent with microscopic observations of infected eye cryosections in which, for both HSV-1 and -2 infected mice, it was possible to detect a considerable virus presence within the cornea scraped for virus challenge. Interestingly, in IgG#33-treated eyes, large amounts of virus were constrained to primary infection site but very low detectable viruses were present within the retina and adjacent eye tissue layers. In contrast, very high amount of virus was present in cornea, retina and other eye tissue layers within the eye receiving IgG mock control, suggesting that unrelated IgG cannot block the spread of infection from cornea to adjacent tissues. This last observation is coherent with clinical depiction of eye disease scoring. Kidneys were dissected and stained in order to establish virus presence and tissue architecture in the different mice cohorts. Kidneys were chosen for immunohistochemistry because in this systemic infection model their evaluation in terms of both virus presence and tissue integrity provides insights related to antiviral/protective activity of the mAb during disseminated HSV infection. Last, kidneys can be explanted without damaging tissue integrity, differently for other organs such as brain that, in the case of last stage HSV-CNS involvement, completely loses its tissue consistency strongly impairing the sample cryosectioning. Confocal microscopy analysis of kidney cryosections revealed that only kidneys explanted from mouse receiving IgG#33 retained tissue integrity, with no evidence of virus in all internal kidney compartments. This observation is fully consistent with the total lack of severe systemic signs of HSV infection in mice treated with IgG#33.

Together, these observations confirmed the potential for IgG#33 as a therapeutic for HSV infection, considering also that in humans the Fc-mediated effects could further improve IgG efficacy allowing for example the recruitment of cellular immunity, such as CD8+ T cells, which play pivotal roles in clearing HSV dissemination (van Lint et al., 2004). These data pave the way for

further studies investigating either the ability of IgG#33 to inhibit virus reactivations *in vivo*, or the presence of gD epitopes eliciting *in vivo* an IgG#33-like antibody response (Belshe et al., 2012; Cairns et al., 2014; Clementi et al., 2017; 2013).

Acknowledgments: Thanks to Fanny Lucchesi from Centro Retrovirus Università di Pisa, for technical support in mice experiments. We would like to thank Dr. R. Santangelo (Department of Microbiology, Università Cattolica del Sacro Cuore of Rome, Italy) for providing HSV-1 and HSV-2 clinical isolates. Experiments employing IN Cell Analyzer 1000 System, Leica Confocal SP2 Microscope and Zeiss Axio Observer.Z1 Microscope with QImaging Exi-Blue were carried out in ALEMBIC, an advanced microscopy laboratory facility established by the San Raffaele Scientific Institute and the Vita-Salute San Raffaele University.

Funding: This work was partially supported by Polichem SA, Lugano, Switzerland. The founders had no role in study design, data collection and analysis, decision to publish, or preparation of the manuscript.

Potential competing interests: RB, MC and DC are listed as inventors on a patent application of human monoclonal antibodies against HSV-1 and -2 for the treatment of HSV diseases. FM is an employee of Polichem SA Lugano, Switzerland. The remaining authors, including the corresponding author, declare no competing interests.

Supplementary data list

- Supplemental Materials and Methods
- Fig. S1. ELISA assays
- Fig. S2. Binding studies performed on HSV infected cells.
- Fig. S3. Fab#33 target identification.
- Fig. S4. Neutralisation assays performed using two techniques.

- Fig. S5. Neutralising activity of different Hu-mAb#33 engineered formats.
- Fig. S6. Neutralising activity of IgG#33 vs HSV clinical isolates featuring different susceptibility to ACV *in vitro*.
- Fig. S7. Post-virus entry assays.
- Fig. S8. Plaque assays.
- Fig. S9. Phenotypic assay on Vero E6 cells for evaluation of acyclovir susceptibility of different HSV-1 and HSV-2 clinical isolates.
- Fig. S10. LD₅₀ for HSV-1 and HSV-2 in all experimental settings.
- Fig. S11. Immunohistochemical analysis of HSV-2 infected mice eyes after sacrifice.
- Fig. S12. Post virus attachment assay.
- Fig. S13. gD1 and gD2 amino acid sequences alignment.

REFERENCES

- Andrei, G., Snoeck, R., 2013. Herpes simplex virus drug-resistance. *Current Opinion in Infectious Diseases* 26, 551–560. doi:10.1097/QCO.0000000000000015
- Atanasiu, D., Cairns, T.M., Whitbeck, J.C., Saw, W.T., Rao, S., Eisenberg, R.J., Cohen, G.H., 2013. Regulation of herpes simplex virus gB-induced cell-cell fusion by mutant forms of gH/gL in the absence of gD and cellular receptors. *MBio* 4. doi:10.1128/mBio.00046-13
- Belshe, R.B., Leone, P.A., Bernstein, D.I., Wald, A., Levin, M.J., Stapleton, J.T., Gorfinkel, I., Morrow, R.L.A., Ewell, M.G., Stokes-Riner, A., Dubin, G., Heineman, T.C., Schulte, J.M., Deal, C.D., Herpevac Trial for Women, 2012. Efficacy results of a trial of a herpes simplex vaccine. *N. Engl. J. Med.* 366, 34–43. doi:10.1056/NEJMoa1103151
- Berdugo, M., Larsen, I.V., Abadie, C., Deloche, C., Kowalczyk, L., Touchard, E., Dubielzig, R., Brandt, C.R., Behar-Cohen, F., Combette, J.M., 2012. Ocular Distribution, Spectrum of Activity, and In Vivo Viral Neutralization of a Fully Humanized Anti-Herpes Simplex Virus IgG Fab Fragment following Topical Application. *Antimicrobial Agents and Chemotherapy* 56, 1390–1402. doi:10.1128/AAC.05145-11
- Burioni, R., Williamson, R.A., Sanna, P.P., Bloom, F.E., Burton, D.R., 1994. Recombinant human Fab to glycoprotein D neutralizes infectivity and prevents cell-to-cell transmission of herpes simplex viruses 1 and 2 in vitro. *Proc. Natl. Acad. Sci. U.S.A.* 91, 355–359.
- Cairns, T.M., Huang, Z.-Y., Whitbeck, J.C., Ponce-de-Leon, M., Lou, H., Wald, A., Krummenacher, C., Eisenberg, R.J., Cohen, G.H., 2014. Dissection of the Antibody Response against Herpes Simplex Virus Glycoproteins in Naturally Infected Humans. *Journal of Virology* 88, 12612–

12622. doi:10.1128/JVI.01930-14

- Chen, J., Davé, S.K., Simmons, A., 2004. Prevention of genital herpes in a guinea pig model using a glycoprotein D-specific single chain antibody as a microbicide. *Viol. J.* 1, 11. doi:10.1186/1743-422X-1-11
- Cherpes, T.L., Matthews, D.B., Maryak, S.A., 2012. Neonatal herpes simplex virus infection. *Clin Obstet Gynecol* 55, 938–944. doi:10.1097/GRF.0b013e31827146a7
- Chiappesi, F., Vannucci, L., De Luca, A., Lai, M., Matteoli, B., Freer, G., Manservigi, R., Ceccherini-Nelli, L., Maggi, F., Bendinelli, M., Pistello, M., 2012. A lentiviral vector-based, herpes simplex virus 1 (HSV-1) glycoprotein B vaccine affords cross-protection against HSV-1 and HSV-2 genital infections. *Journal of Virology* 86, 6563–6574. doi:10.1128/JVI.00302-12
- Clementi, N., Cappelletti, F., Criscuolo, E., Castelli, M., Mancini, N., Burioni, R., Clementi, M., 2017. Role and potential therapeutic use of antibodies against herpetic infections. *Clinical Microbiology and Infection* 1–19. doi:10.1016/j.cmi.2016.12.023
- Clementi, N., Criscuolo, E., Cappelletti, F., Burioni, R., Clementi, M., Mancini, N., 2016. Novel therapeutic investigational strategies to treat severe and disseminated HSV infections suggested by a deeper understanding of in vitro virus entry processes. *Drug Discov. Today*. doi:10.1016/j.drudis.2016.03.003
- Clementi, N., Criscuolo, E., Castelli, M., Clementi, M., 2012. Broad-range neutralizing anti-influenza A human monoclonal antibodies: new perspectives in therapy and prophylaxis. *New Microbiol.* 35, 399–406.
- Clementi, N., Mancini, N., Castelli, M., Clementi, M., Burioni, R., 2013. Characterization of epitopes recognized by monoclonal antibodies: experimental approaches supported by freely accessible bioinformatic tools. *Drug Discov. Today* 18, 464–471. doi:10.1016/j.drudis.2012.11.006
- Cohen, G.H., Isola, V.J., Kuhns, J., Berman, P.W., Eisenberg, R.J., 1986. Localization of discontinuous epitopes of herpes simplex virus glycoprotein D: use of a non-denaturing (“native” gel) system of polyacrylamide gel electrophoresis coupled with Western blotting. *Journal of Virology* 60, 157–166.
- Däumer, M.P., Schneider, B., Giesen, D.M., Aziz, S., Kaiser, R., Kupfer, B., Schneweis, K.E., Schneider-Mergener, J., Reineke, U., Matz, B., Eis-Hübinger, A.M., 2011. Characterisation of the epitope for a herpes simplex virus glycoprotein B-specific monoclonal antibody with high protective capacity. *Med. Microbiol. Immunol.* 200, 85–97. doi:10.1007/s00430-010-0174-x
- De Logu, A., Williamson, R.A., Rozenshteyn, R., Ramiro-Ibañez, F., Simpson, C.D., Burton, D.R., Sanna, P.P., 1998. Characterization of a type-common human recombinant monoclonal antibody to herpes simplex virus with high therapeutic potential. *J. Clin. Microbiol.* 36, 3198–3204.
- Dimmock, N.J., 1993. Neutralization of animal viruses. *Curr. Top. Microbiol. Immunol.* 183, 1–149.
- Gallagher, J.R., Atanasiu, D., Saw, W.T., Paradisgarten, M.J., Whitbeck, J.C., Eisenberg, R.J., Cohen, G.H., 2014. Functional Fluorescent Protein Insertions in Herpes Simplex Virus gB Report on gB Conformation before and after Execution of Membrane Fusion. *PLoS Pathog* 10, e1004373. doi:10.1371/journal.ppat.1004373
- Gallagher, J.R., Saw, W.T., Atanasiu, D., Lou, H., 2013. Displacement of the C terminus of herpes simplex virus gD is sufficient to expose the fusion-activating interfaces on gD. *Journal of ...*
- Galluccio, E., Cassina, L., Russo, I., Gelmini, F., Setola, E., Rampoldi, L., Citterio, L., Rossodivita, A., Kamami, M., Colombo, A., Alfieri, O., Carini, M., Bosi, E., Trovati, M., Piatti, P., Monti, L.D., Casari, G., 2014. A novel truncated form of eNOS associates with altered vascular function. *Cardiovasc. Res.* 101, 492–502. doi:10.1093/cvr/cvt267
- Gianni, T., Massaro, R., Campadelli-Fiume, G., 2015. Dissociation of HSV gL from gH by $\alpha\beta 6$ - or

- $\alpha\beta 8$ -integrin promotes gH activation and virus entry. *Proc. Natl. Acad. Sci. U.S.A.* 201506846–14. doi:10.1073/pnas.1506846112
- Gilbert, C., Bestman-Smith, J., Boivin, G., 2002. Resistance of herpesviruses to antiviral drugs: clinical impacts and molecular mechanisms. *Drug Resist. Updat.* 5, 88–114.
- Glassman, P.M., Balthasar, J.P., 2014. Mechanistic considerations for the use of monoclonal antibodies for cancer therapy. *Cancer Biol Med* 11, 20–33. doi:10.7497/j.issn.2095-3941.2014.01.002
- Grinde, B., 2013. Herpesviruses: latency and reactivation – viral strategies and host response. *Journal of Oral Microbiology* 5, 283–9. doi:10.3402/jom.v5i0.22766
- Jackson, J.O., Lin, E., Spear, P.G., Longnecker, R., 2010. Insertion mutations in herpes simplex virus 1 glycoprotein H reduce cell surface expression, slow the rate of cell fusion, or abrogate functions in cell fusion and viral entry. *Journal of Virology* 84, 2038–2046. doi:10.1128/JVI.02215-09
- Jefferis, R., 2012. Isotype and glycoform selection for antibody therapeutics. 526, 159–166. doi:10.1016/j.abb.2012.03.021
- Johnston, C., Koelle, D.M., Wald, A., 2011. HSV-2: in pursuit of a vaccine. *J. Clin. Invest.* 121, 4600–4609. doi:10.1172/JCI57148
- Knox, S.J., Levy, R., Hodgkinson, S., Bell, R., Brown, S., Wood, G.S., Hoppe, R., Abel, E.A., Steinman, L., Berger, R.G., 1991. Observations on the effect of chimeric anti-CD4 monoclonal antibody in patients with mycosis fungoides. *Blood* 77, 20–30.
- Krawczyk, A., Arndt, M.A.E., Grosse-Hovest, L., Weichert, W., Giebel, B., Dittmer, U., Hengel, H., Jäger, D., Schneewis, K.E., Eis-Hübinger, A.M., Roggendorf, M., Krauss, J., 2013. Overcoming drug-resistant herpes simplex virus (HSV) infection by a humanized antibody. *Proc. Natl. Acad. Sci. U.S.A.* 110, 6760–6765. doi:10.1073/pnas.1220019110
- Krawczyk, A., Dirks, M., Kasper, M., Buch, A., Dittmer, U., Giebel, B., Wildschütz, L., Busch, M., Goergens, A., Schneewis, K.E., Eis-Hübinger, A.M., Sodeik, B., Heiligenhaus, A., Roggendorf, M., Bauer, D., 2015. Prevention of Herpes Simplex Virus Induced Stromal Keratitis by a Glycoprotein B-Specific Monoclonal Antibody. *PLoS ONE* 10, e0116800–24. doi:10.1371/journal.pone.0116800
- Lascaux, A.-S., Caumes, E., Deback, C., Melica, G., Challine, D., Agut, H., Lévy, Y., 2012. Successful treatment of aciclovir and foscarnet resistant Herpes simplex virus lesions with topical imiquimod in patients infected with human immunodeficiency virus type 1. *J. Med. Virol.* 84, 194–197. doi:10.1002/jmv.23188
- Lazear, E., Whitbeck, J.C., Ponce-de-Leon, M., Cairns, T.M., Willis, S.H., Zuo, Y., Krummenacher, C., Cohen, G.H., Eisenberg, R.J., 2012. Antibody-induced conformational changes in herpes simplex virus glycoprotein gD reveal new targets for virus neutralization. *Journal of Virology* 86, 1563–1576. doi:10.1128/JVI.06480-11
- Lee, C.-C., Lin, L.-L., Chan, W.-E., Ko, T.-P., Lai, J.-S., Wang, A.H.-J., 2013. Structural basis for the antibody neutralization of Herpes simplex virus. *Acta Crystallogr. D Biol. Crystallogr.* 69, 1935–1945. doi:10.1107/S0907444913016776
- Looker, K.J., Magaret, A.S., Turner, K.M.E., Vickerman, P., Gottlieb, S.L., Newman, L.M., 2015. Global Estimates of Prevalent and Incident Herpes Simplex Virus Type 2 Infections in 2012. *PLoS ONE* 10, e114989. doi:10.1371/journal.pone.0114989
- Marasco, W.A., Sui, J., 2007. The growth and potential of human antiviral monoclonal antibody therapeutics. *Nat Biotechnol* 25, 1421–1434. doi:10.1038/nbt1363
- Minson, A.C., Hodgman, T.C., Digard, P., Hancock, D.C., Bell, S.E., Buckmaster, E.A., 1986. An analysis of the biological properties of monoclonal antibodies against glycoprotein D of herpes simplex virus and identification of amino acid substitutions that confer resistance to

- neutralization. *J. Gen. Virol.* 67 (Pt 6), 1001–1013. doi:10.1099/0022-1317-67-6-1001
- Muggeridge, M.I., Wu, T.T., Johnson, D.C., Glorioso, J.C., Eisenberg, R.J., Cohen, G.H., 1990. Antigenic and functional analysis of a neutralization site of HSV-1 glycoprotein D. *Virology* 174, 375–387.
- Nicola, A.V., Ponce de Leon, M., Xu, R., Hou, W., Whitbeck, J.C., Krummenacher, C., Montgomery, R.I., Spear, P.G., Eisenberg, R.J., Cohen, G.H., 1998. Monoclonal antibodies to distinct sites on herpes simplex virus (HSV) glycoprotein D block HSV binding to HVEM. *Journal of Virology* 72, 3595–3601.
- Perotti, M., Mancini, N., Diotti, R.A., Tarr, A.W., Ball, J.K., Owsianka, A., Adair, R., Patel, A.H., Clementi, M., Burioni, R., 2008. Identification of a broadly cross-reacting and neutralizing human monoclonal antibody directed against the hepatitis C virus E2 protein. *Journal of Virology* 82, 1047–1052. doi:10.1128/JVI.01986-07
- Presta, L.G., 2006. Engineering of therapeutic antibodies to minimize immunogenicity and optimize function. *Adv. Drug Deliv. Rev.* 58, 640–656. doi:10.1016/j.addr.2006.01.026
- Ranade, A.R., Wilson, M.S., McClanahan, A.M., Ball, A.J., 2014. High Content Imaging and Analysis Enable Quantitative In Situ Assessment of CYP3A4 Using Cryopreserved Differentiated HepaRG Cells. *J Toxicol* 2014, 291054–12. doi:10.1155/2014/291054
- Sanna, P.P., De Logu, A., Williamson, R.A., Hom, Y.L., Straus, S.E., Bloom, F.E., Burton, D.R., 1996. Protection of nude mice by passive immunization with a type-common human recombinant monoclonal antibody against HSV. *Virology* 215, 101–106. doi:10.1006/viro.1996.0011
- Sanna, P.P., Deerinck, T.J., Ellisman, M.H., 1999. Localization of a passively transferred human recombinant monoclonal antibody to herpes simplex virus glycoprotein D to infected nerve fibers and sensory neurons in vivo. *Journal of Virology* 73, 8817–8823.
- Sanna, P.P., Ramiro-Ibañez, F., De Logu, A., 2000. Synergistic interactions of antibodies in rate of virus neutralization. *Virology* 270, 386–396. doi:10.1006/viro.2000.0276
- Sanna, P.P., Williamson, R.A., De Logu, A., Bloom, F.E., Burton, D.R., 1995. Directed selection of recombinant human monoclonal antibodies to herpes simplex virus glycoproteins from phage display libraries. *Proc. Natl. Acad. Sci. U.S.A.* 92, 6439–6443.
- Schubert, A., Gentner, E., Bohn, K., Schwarz, M., Mertens, T., Sauerbrei, A., 2014. Single nucleotide polymorphisms of thymidine kinase and DNA polymerase genes in clinical herpes simplex virus type 1 isolates associated with different resistance phenotypes. *Antiviral Res.* 107, 16–22. doi:10.1016/j.antiviral.2014.03.015
- Solfrosi, L., Mancini, N., Canducci, F., Clementi, N., Sautto, G.A., Diotti, R.A., Clementi, M., Burioni, R., 2012. A phage display vector optimized for the generation of human antibody combinatorial libraries and the molecular cloning of monoclonal antibody fragments. *New Microbiol.* 35, 289–294.
- Stampfer, S.D., Lou, H., Cohen, G.H., Eisenberg, R.J., Heldwein, E.E., 2010. Structural basis of local, pH-dependent conformational changes in glycoprotein B from herpes simplex virus type 1. *Journal of Virology* 84, 12924–12933. doi:10.1128/JVI.01750-10
- Superti, F., Ammendolia, M.G., Marchetti, M., 2008. New advances in anti-HSV chemotherapy. *Curr. Med. Chem.* 15, 900–911.
- Teepe, A.G., Allen, L.B., Wordinger, R.J., Harris, E.F., 1990. Effect of the estrous cycle on susceptibility of female mice to intravaginal inoculation of herpes simplex virus type 2 (HSV-2). *Antiviral Res.* 14, 227–235.
- Tognon, M., Manservigi, R., Sebastiani, A., Bragliani, G., Busin, M., Cassai, E., 1985. Analysis of HSV isolated from patients with unilateral and bilateral herpetic keratitis. *Int Ophthalmol* 8, 13–18.
- Vahne, A., Svennerholm, B., Sandberg, M., Hamberger, A., Lycke, E., 1980. Differences in attachment between herpes simplex type 1 and type 2 viruses to neurons and glial cells.

Infect. Immun. 28, 675–680.

- van Lint, A., Ayers, M., Brooks, A.G., Coles, R.M., Heath, W.R., Carbone, F.R., 2004. Herpes simplex virus-specific CD8+ T cells can clear established lytic infections from skin and nerves and can partially limit the early spread of virus after cutaneous inoculation. *J. Immunol.* 172, 392–397. doi:10.4049/jimmunol.172.1.392
- Whitley, R.J., 2006. Herpes simplex encephalitis: adolescents and adults. *Antiviral Res.* 71, 141–148. doi:10.1016/j.antiviral.2006.04.002
- Whitley, R.J., Roizman, B., 2001. Herpes simplex virus infections. *The Lancet* 357, 1513–1518. doi:10.1016/S0140-6736(00)04638-9
- Zeitlin, L., Olmsted, S.S., Moench, T.R., Co, M.S., Martinell, B.J., Paradkar, V.M., Russell, D.R., Queen, C., Cone, R.A., Whaley, K.J., 1998. A humanized monoclonal antibody produced in transgenic plants for immunoprotection of the vagina against genital herpes. *Nat Biotechnol* 16, 1361–1364. doi:10.1038/4344
- Zeitlin, L., Whaley, K.J., Sanna, P.P., Moench, T.R., Bastidas, R., De Logu, A., Williamson, R.A., Burton, D.R., Cone, R.A., 1996. Topically applied human recombinant monoclonal IgG1 antibody and its Fab and F(ab')₂ fragments protect mice from vaginal transmission of HSV-2. *Virology* 225, 213–215.

FIGURES and CAPTIONS

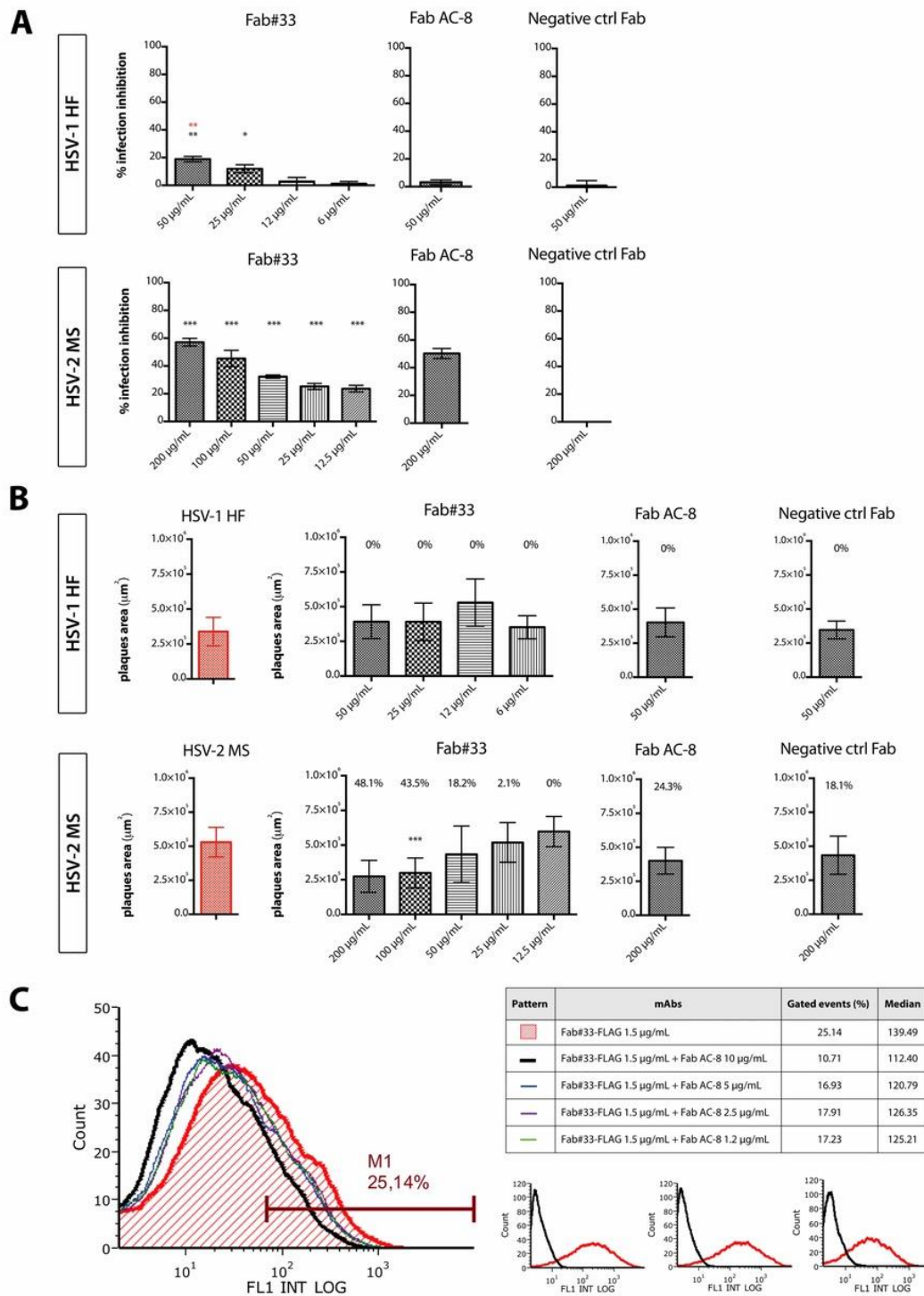
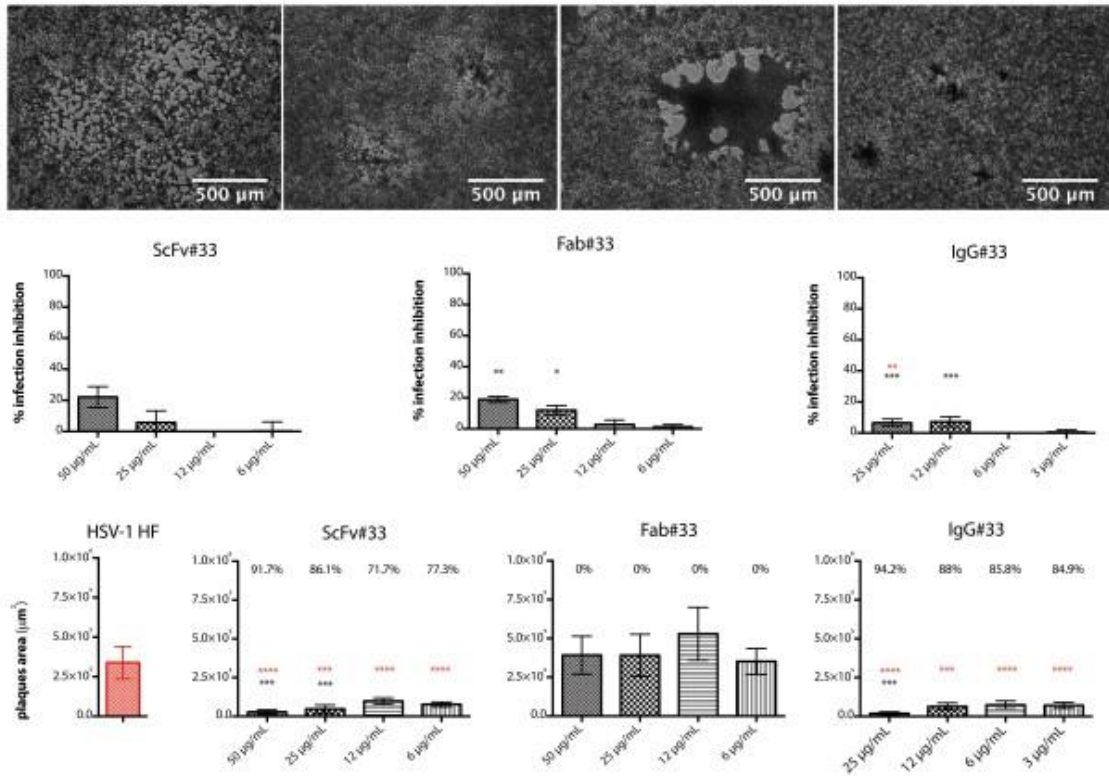


Fig. 1. Post-virus entry inhibition assays. (A) Evaluation of the ability of **Fab#33** to decrease number of plaques compared to both HSV-1 HF and HSV-2 MS virus positive control in “post-entry assays”. (B) Evaluation of mean plaque area reduction for **Fab#33** treated cells previously infected

with either HSV-1 HF or HSV-2 MS. Controls (AC-8 and unrelated negative control Fab) are included for all experiments. Percent reduction compared to the infection control is reported above each column (statistically significant p values obtained by comparing Fab#33 to Fab mock control, black asterisks, and Fab AC-8, red asterisks, *** $p < 0.001$, ** $p < 0.01$). (C) Competition assay between Fab#33-FLAG and Fab AC-8 performed by FACS analysis of cells transfected with gD1. The table shows the differences in the number of gated cells and median due to competition between the two Fabs. Below, the signal controls of the different antibodies on gD1 transfected cells (red) and negative cells (black), in order: commercial anti-gD1 control, Fab#33-FLAG, Fab AC-8.

A



B

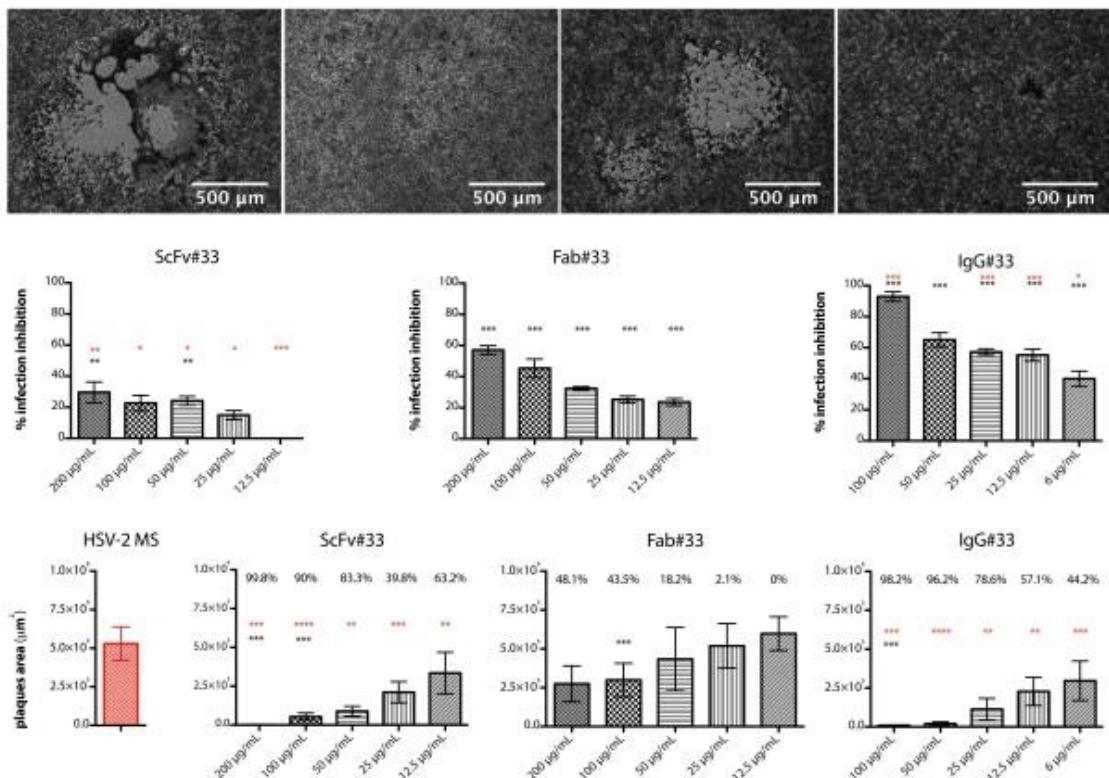


Fig. 2. Post-entry assays for the comparison of inhibitory activity of scFv#33, Fab#33 and IgG#33.

Bright-field optical microscopy pictures collected for cells treated with the three antibody formats.

Bar 500 μm , magnification 5x. Columns (left to right) show respectively virus positive infection controls and the three engineered mAb formats (*scFv#33*, *Fab#33* and *IgG#33*). Inhibition of plaque number is indicated on second rows as “% infection inhibition” compared to an uninhibited positive area control. Third rows depict plaque area means (expressed in μm^2) and upper and lower 95% CI from mean (above each column, the percentages indicating plaque area reduction compared to virus control is indicated). *Hu-mAb#33* engineered molecular formats tested against HSV-1 HF (A) and HSV-2 MS (B). (statistically significant *p* values obtained by comparing mAb#33 to mAb mock control, black asterisks, and Fab#33 to IgG#33 or scFv#33, red asterisks, *****p*<0.0001, ****p*<0.001, ***p*<0.01, **p*<0.05).

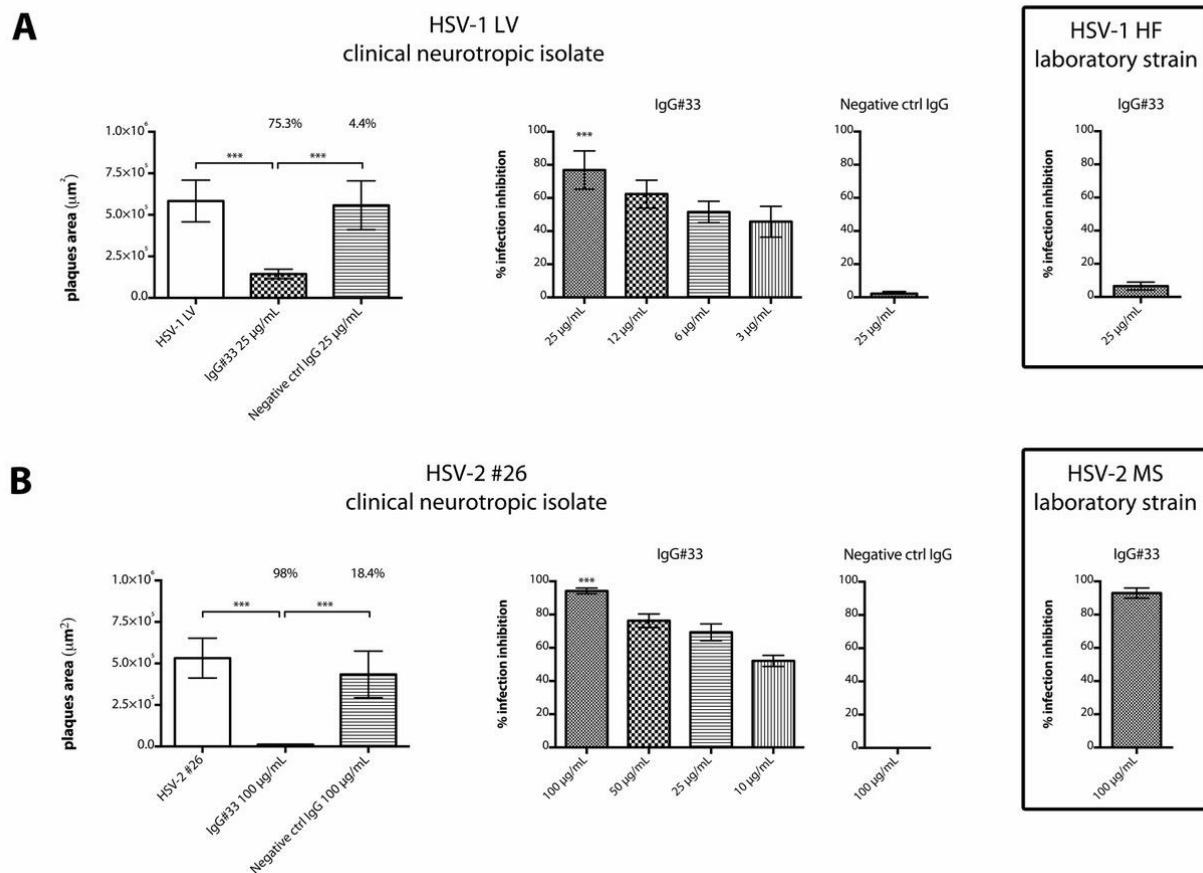


Fig. 3. Evaluation of the ability of *IgG#33* to inhibit replication of clinical HSV isolates after virus entry. Both LV (HSV-1, panel A) and #26 (HSV-2, panel B) clinical isolates were efficiently inhibited

by IgG#33 in *in vitro* post-virus entry assays. IgG#33 reduced both area and number of plaques compared to positive infection controls. From left to right: inhibition of plaque area by IgG#33. Mean of areas (\pm 95% CI) measured on differently treated infected cells are indicated. The values reported above each column indicate percentage reduction in plaque area compared to virus control. Then, inhibition of plaque number by IgG#33. Plaque number was compared to positive infection controls in the absence of inhibitor. A single concentration was used to compare the activity of IgG#33 against HSV clinical isolates (black boxes). (p-values obtained comparing IgG#33 to mAb mock control, *** $p < 0.001$).

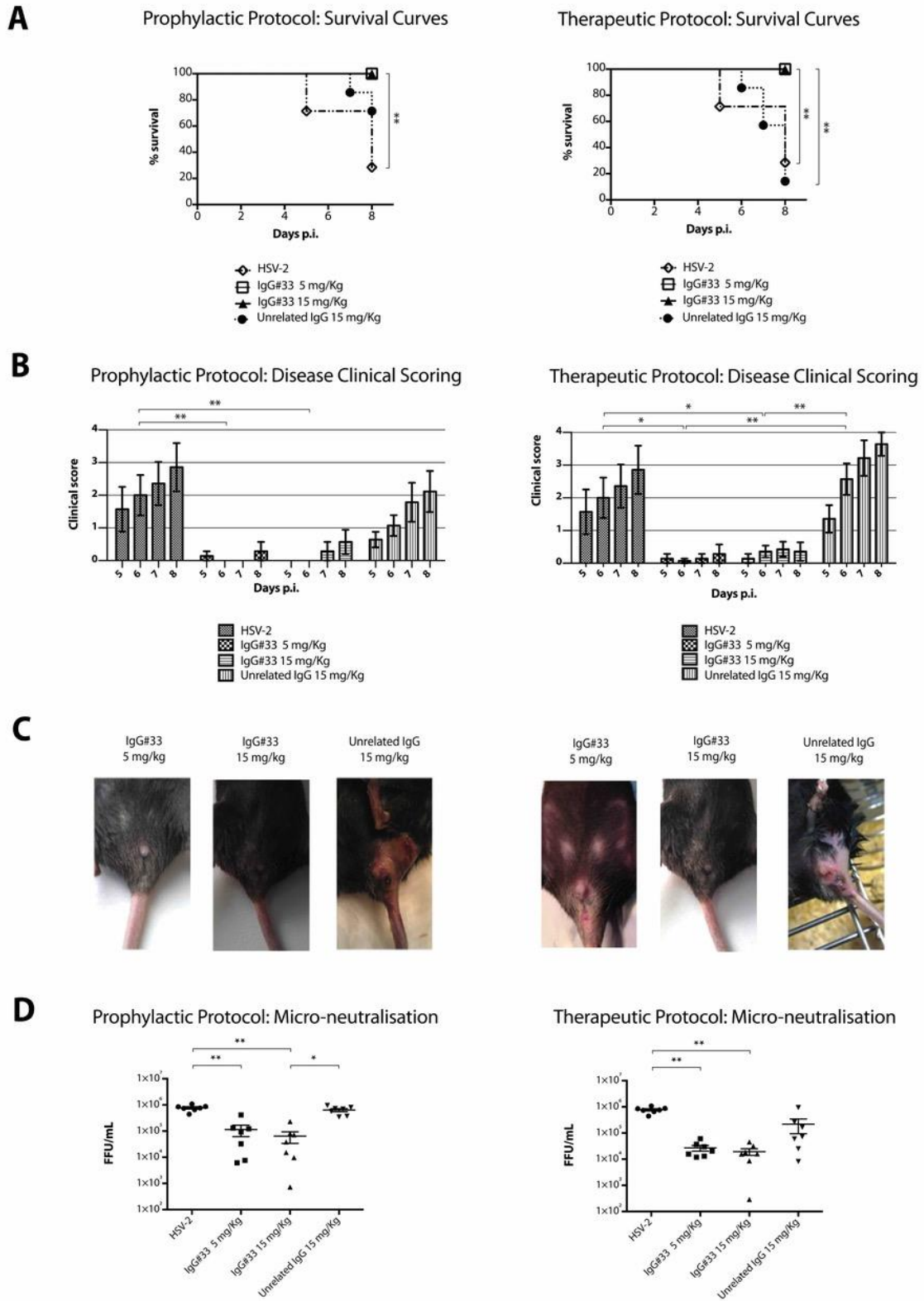


Fig. 4. Prophylactic and therapeutic activity of a single systemic injection of IgG#33 against HSV-2 vaginal challenge. (A) Survival curves of the different treated groups (** $p < 0.01$). (B) Clinical disease scoring indicated the mean index of clinical disease in the different mice groups, from day

5 to 8 p.i. Error bars within the graph indicate SEM (** $p < 0.01$, * $p < 0.05$). (C) Pictures taken at 8th day p.i. show examples of clinical presentation of mice receiving intravaginal HSV-2 challenge. (D) IN Cell Analyzer System analysis indicates the titres detected in vaginal lavages collected 48h p.i. Means and SEM for each group of mice are indicated (** $p < 0.01$, * $p < 0.05$).

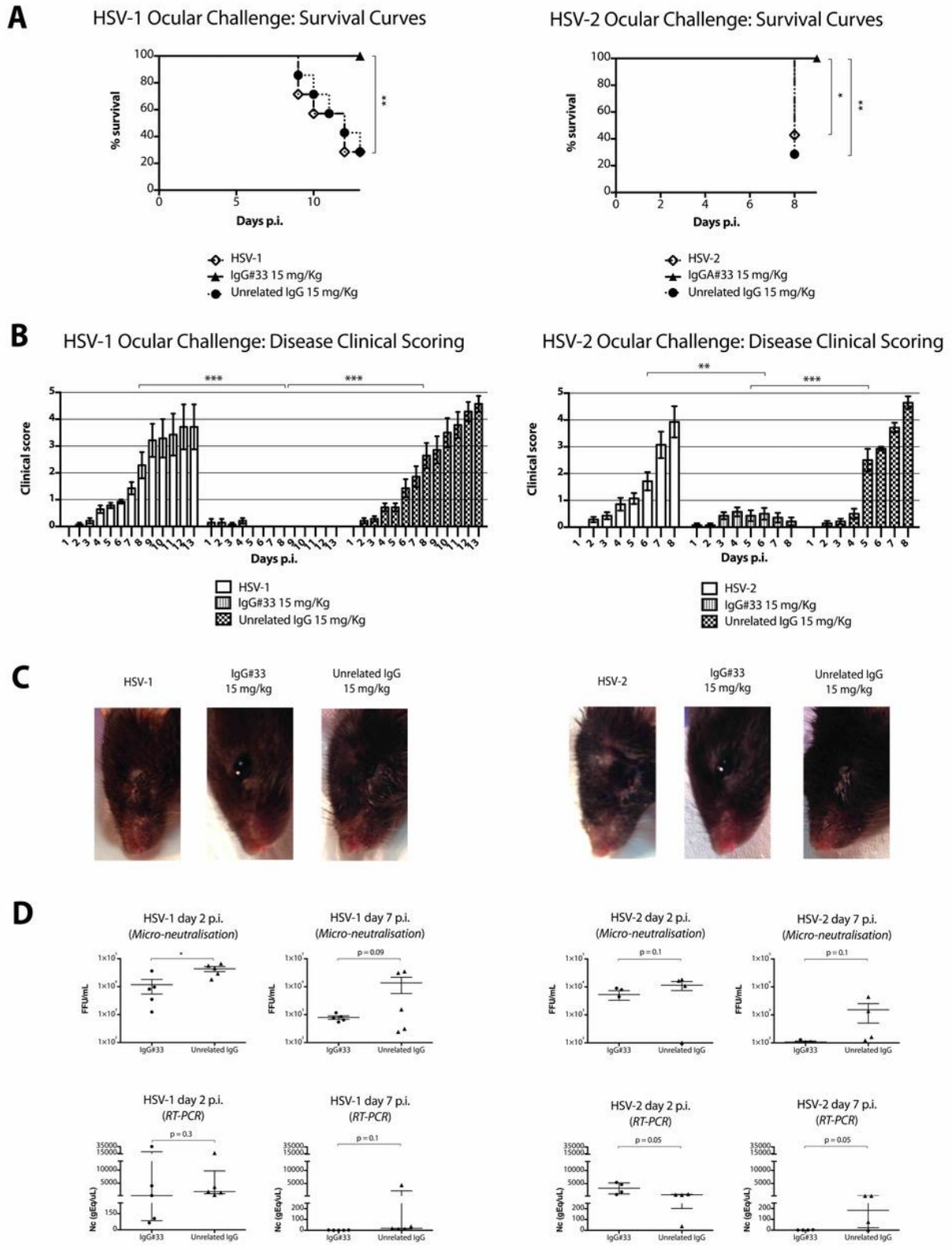


Fig. 5. Therapeutic activity of a single systemic injection of IgG#33 against both HSV-1 and HSV-2 ocular virus challenge. (A) Survival curves of the different treated groups (** $p < 0.01$, * $p < 0.05$). (B) Mean clinical disease scoring for all mice receiving different drug-regimens, from day 1 to 13 p.i.

and 1 to 8 p.i. for mice challenged with HSV-1 and HSV-2 respectively. SEM of the clinical scoring for each group is presented ($***p<0.001$, $**p<0.01$). (C) Images taken at day 7 p.i. highlight examples of clinical presentation of mice receiving ocular HSV-1 and HSV-2 challenge. (D) Graphs reporting IN Cell Analyzer System analysis and RT-PCR analysis indicated the titres in film tear lavages collected at day 2 and day 7 p.i., and the virus genome load for the same samples, respectively. The median viral titre/viral load with interquartile range is reported for each group ($*p<0.05$).

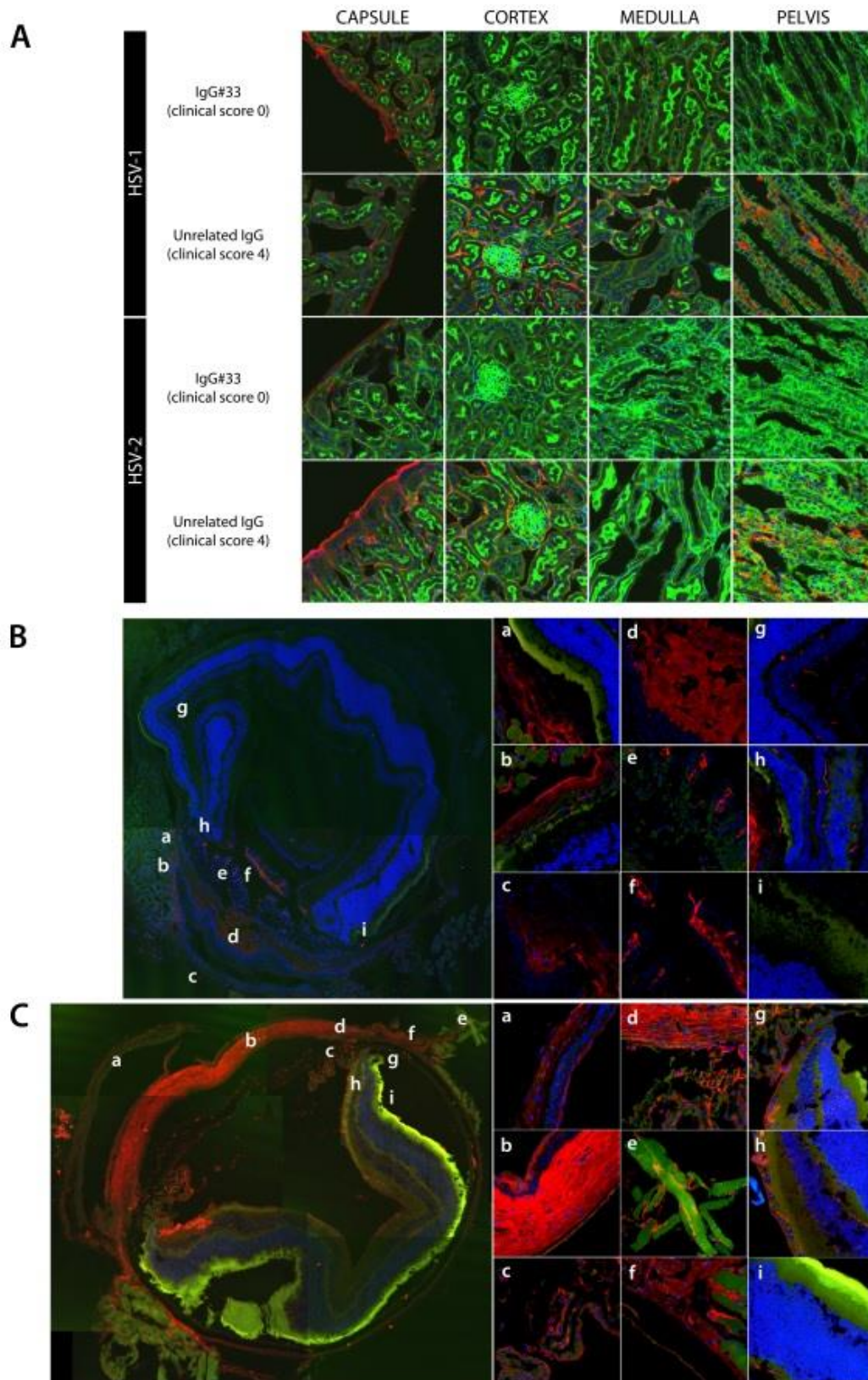


Fig. 6. Immunohistochemical analysis of mouse tissues (A) Imaging of kidney sections after mouse sacrifice. Images (63-fold magnification) highlight different kidney cryosections (capsule, cortex, medulla and pelvis). Green fluorescence highlights F-actin bound by Phalloidin Alexa Fluor 488®,

red signal (anti-HSV1 + HSV2 gD antibody Alexa Fluor 546[®]) indicates virus presence and blue Hoechst signal highlights nuclei. For each row the virus used to perform the challenge, the treatment regimen and the clinical scoring of dissected animals are indicated. (B, C)

Immunohistochemical analysis of HSV-1 infected mouse eyes after sacrifice. Ten-fold magnification pictures (merged images), displayed on the left, present an overview of the whole eye cryosection (lens axis). Panels (63-fold magnification) show different details of eyes. Green fluorescence highlights F-actin bound by Phalloidin Alexa Fluor 488[®] and red signal of anti-HSV1 + HSV2 gD antibody (Alexa Fluor 546[®]) indicates virus presence, blue Hoechst signal indicates nuclei.

(B) Eye dissected from mouse receiving single systemic administration of [IgG#33](#) (15mg/Kg). Panels indicate: extraocular muscles, corneal and conjunctive detached tissues, a and b; cornea and conjunctive, c and d; iris and ocular anterior chamber, e and f; retina, g to i. (C) Eye dissected from unrelated IgG (15mg/Kg) receiving mouse systemically administered after infection. Panels indicate: cornea and conjunctive, a and b; iris and ocular anterior chamber, c and d; extraocular muscles, corneal tissues, e and f; retina, g to i.

SUPPLEMENTAL FILES

Materials and Methods

Cells and Viruses. Vero E6 (Vero C1008, clone E6 - ATCC[®] CRL-1586[™]) and HEK 293T (ATCC[®] CRL-1586[™]) cells were both cultured in Dulbecco's Modified Eagle Medium (Gibco[®] DMEM, ThermoFisher Scientific) containing 10% (v/v) fetal bovine serum (FCS, EuroClone), 100 U/mL penicillin and 0.1 mg/mL streptomycin (Gibco[®] ThermoFisher Scientific), 0.01 M HEPES (Gibco[®] ThermoFisher Scientific) and MEM Non-Essential Amino Acids (Gibco[®] ThermoFisher Scientific). The laboratory strains HSV-1 HF (ATCC[®] VR-260[™]) and HSV-2 MS (ATCC[®] VR-540[™]) were used. Clinical isolates HSV-1 #1 (oral cavity), #7 (bronchoalveolar lavage, BAL), #8 (pharyngeal swab) and #11 (vesicle), and HSV-2 #18 (cutaneous swab), #21 (vaginal discharge), #25 (vaginal swab), #26 and #28 (both cutaneous swab) were kindly provided by Dr. R. Santangelo, Department of Microbiology, Università Cattolica del Sacro Cuore of Rome, Italy. HSV-1 LV neurovirulent strain has been described elsewhere (Tognon et al., 1985). **(i) *In vitro* virus propagation and titration.** These strains were expanded in semiconfluent T-25 flasks (Corning[®] CellBIND[®]) of Vero E6 cells. The cells were infected with HSV-1 or HSV-2 in complete DMEM without FBS, and after 2 h the medium was replaced with fresh complete DMEM with 2% FBS, and cultured for further 2 to 3 days until cell lysis. Cell supernatants were then collected and, after clarification at 800 x g for 5 min, stored in small aliquots at -80°C until use. For examination of virus titers the cell supernatants were tested on Vero E6 monolayers using plaque assay or IN Cell Analyzer System analysis (GE Healthcare IN Cell Analyzer 1000 System). Plaque titration of the viral stocks was carried out seeding the cells (1×10^5 /well) in 24-well plates and the next day inoculated with 10-fold dilutions (range, 10^{-2} to 10^{-6}) of the viral stocks in duplicate. After 20 min, the medium was replaced with complete DMEM with 2% FBS and 1% Agarose (BD BaculoGold[™] Plaque Assay Agarose) and the plates were incubated for 46 h. The cells were then fixed with 4% formaldehyde

solution in PBS for 1 h and stained with crystal violet, and viral plaques were counted. Titers are expressed as PFU/mL. IN Cell Analyzer System analysis of the viral stocks instead was carried out seeding Vero E6 cells (2.6×10^4 /well) in 96-well plates and the next day inoculated with 10-fold dilutions (range, 10^{-1} to 10^{-8}) of the viral stocks in triplicate. After 2 h, the medium was replaced with complete DMEM with 2% FBS and the plates were incubated for 21 h. The cells were then fixed with 1:1 solution of acetone/methanol and stained. Briefly, anti-HSV1 + HSV2 gD antibody [2C10] (ab6507, Abcam) and Goat anti-Mouse IgG (whole molecule)-FITC antibody (F0257, Sigma-Aldrich) were used as primary and secondary antibody, respectively. Hoechst 33258 (Sigma-Aldrich) was used for nuclear staining. Then IN Cell Analyzer System allowed high throughput acquisition of high quality images of the plates and its software counted the fraction of infected cells of each well. Titres are expressed as 50% Tissue culture Infective Dose (TCID₅₀)/mL. **(ii) *In vivo* viral inoculum effect.** Since age and oestrous cycle are known to influence the susceptibility to genital, *in vivo* titration via vaginal challenge of HSV-2 MS viral stock was performed in mice at 11 weeks of age, with their oestrous cycles synchronized (Teepe et al., 1990). Cycle synchronization was achieved with 2 mg of depot medroxyprogesterone acetate (Depo-Provera, Pfizer Italia) inoculated subcutaneously 5 days before infection. To facilitate virus absorption, the vaginas were pre-swabbed with a dry-tipped swab immediately prior to the instillation of 10-fold dilutions **in DMEM of the viral stocks, pipetting 50 μ L of virus dilution in mice vaginas** under 2,2,2-tribromoethanol general anaesthesia. The animals were then examined daily for signs of infection. These usually showed up at day 5 or 6 with local erythema and ulcers and rapidly evolved into manifestations of nervous system involvement (arched backs, feeble movements, and paralysis of one or both hind limbs). The latter stage was usually irreversible, and death occurred within 1 to 2 days. HSV-1 LV and HSV-2 MS viral stocks were used for *in vivo* titration via ocular challenge as well. Under 2,2,2-tribromoethanol general anaesthesia, the right cornea was scarified with a

sterile glass Pasteur pipette. Four scratches were made to facilitate virus adsorption (Berduogo et al., 2012). A 5 µL drop of DMEM (2% serum) containing 10-fold dilutions of the viral stocks was applied to the scarified cornea. The eyelids were closed twice over the cornea, and the animals were returned to their cages. The animals were then examined daily for signs of infection as puffy eyelids, crusting, cloudiness, opaque or perforated cornea, swollen shut eye. These symptoms can resolve within few days, but if not they rapidly evolved into manifestations of nervous system involvement (arched backs, altered motor function), an irreversible stage. Animals that survived despite paralysis or other irreversible lesions were euthanized by cervical dislocation under anaesthesia. Thus, the lethal dose 50 (LD₅₀) of both viruses was assessed for either protocols of infection. About 3 LD₅₀ of each virus settings were used in therapeutic and prophylactic experiments. The selected doses of both viruses for the different infection protocols resulted in an irreversible condition at day 8 p.i. for HSV-2 MS (both for vaginal and ocular challenge) and at day 13 p.i. for HSV-1 LV. Mice with mild symptoms or which recovered from disease were followed up for 20 days p.i. and no relevant differences in their conditions were observed.

Patients' sera evaluation for anti HSV reactivity. Sera were collected from 20 patients and tested for the reactivity against HSV-1 and HSV-2 performing an enzyme-linked immunosorbent assay (ELISA). Informed consent was obtained for all patients. Briefly, HSV-1 HF and HSV-2 MS strains were expanded in confluent T-25 flasks (Corning® CellBIND®) of Vero E6 cells. The cells were infected with viruses in complete DMEM without FBS, and after 2 h the medium was replaced with fresh complete DMEM with 2% FBS, and cultured for further 2 to 3 days until cell lysis. Cell supernatants were then collected and, after clarification at 800 x g for 5 min, heat-inactivated for 30 min (HSV-1) or 10 min (HSV-1) at 56°C. Then the supernatants were used for overnight coating of 96-wells microplate (Corning® Costar®) at 4°C. Coating control with 1% Bovine Serum Albumin (BSA, Sigma-Aldrich) solution in PBS was added for not specific reactivity control. The following

day, the plate was blocked with 1% BSA solution in PBS to prevent not specific binding to wells and sera were incubated with antigens for 1 h at 37°C. After washing with 0.1% Tween 20 (Sigma-Aldrich) in PBS solution, detection was with Goat Anti-Human IgG (Fab specific)–Peroxidase antibody (A0293, Sigma-Aldrich) and Pierce™ TMB Substrate Kit (ThermoFisher Scientific). 450 nm Optical Density (O.D.) was measured using Multiskan GO (ThermoFisher Scientific). The patient #18 whose serum showed higher reactivity was chosen for peripheral B cells collection.

Generation and production of an anti-HSV human mAb (Hu-mAb). The preparation of human antibody Fab libraries displayed on the surface of M13 phage has been described (Galanis et al., 2001). Briefly, peripheral B cells mRNAs codifying for Ab HCs and LCs was retro-transcribed in cDNA to construct phagemid library to be converted in phage library and panned for the selection of Fab fragments specific for the selected target. Following these procedures, **Fab#33** was selected from peripheral blood B-lymphocytes of donor showing strong serum IgGs ELISA reactivity against both HSV-1 and 2 virus isolates. Antigens binding phages were selected against HSV-1 and HSV-2 infected Vero E6 after a deselection step against uninfected cells. Phages from the final round of panning procedure were converted to a soluble Fab expressing phagemid system and **Fab#33** was selected for its reactivity against both HSV-1 and HSV-2 infected cells. The antibody was affinity purified from *E. coli* supernatant over a column prepared with a Goat anti-Human IgG F(ab')₂ Secondary Antibody (ThermoFisher Scientific) bound to GammaBind G Sepharose medium (GE Healthcare) as described (Solfrosi et al., 2012).

scFv and IgG#33. Single chain **mAb#33** (scFv) VL/VH was constructed as follows: variable light chain sequence (VL) and variable high chain (VH) sequences of **Fab#33** were amplified using specific primers containing the linker sequence. In brief, **overlapping** primers for VL and VH were designed containing the 15-amino acid (Gly₄Ser)₃ flexible hinge region respectively at 3' and 5'. The scFv sequence containing 3' Hexa-His tag was then cloned into pCM expression vector

FBS, and cultured for further 6 days until complete cell lysis. Cell supernatants were then collected and placed at 56°C for 30 min for virus inactivation. After clarification at 8,000 x g for 10 min at 4°C, the supernatants were loaded on a 5% (w/v) sucrose cushion and centrifuged at 100,000 x g for 1h at 4°C. The pellet containing the virus was then resuspended, loaded on a sucrose gradient (range, 10% to 60%) and centrifuged at 30,000 x g for 5h at 4°C. The purified virus was collected from the interface between 30% and 60% layers. The purified HSV-1 HF was resolved on a SDS-PAGE (Bolt® 4-12% Bis-Tris Plus Gel, ThermoFisher Scientific) and electroblotted onto PVDF membrane in Transfer Buffer (25 mM Tris, 190 mM glycine, 20% methanol, 0.1 % SDS, pH 8.3). Western blot was prepared according to standard protocols. Briefly, blotted PVDF membrane was blocked with 5% non-fat dry milk in Tris-buffered saline (TBS) and probed with Fab#33, anti-HSV1 + HSV2 gD antibody [2C10] and anti-HSV1 + HSV2 gB antibody [10B7] (ab6506, Abcam) in 1% non-fat dry milk in TBS containing 0.1% Tween 20. Detection was with a Goat Anti-Human IgG (Fab specific)–Peroxidase antibody (A0293, Sigma-Aldrich) for Fab#33, and with a Goat Anti-Mouse IgG (whole molecule)–Peroxidase antibody (A4416, Sigma-Aldrich) for control antibodies, and SuperSignal® West Pico Chemiluminescent Substrate (ThermoFisher Scientific).

(ii) HSV-1 gD and gB gene cloning and transient transfection of HEK 293T cells. HSV-1 infected Vero E6 cells supernatant was used for virus DNA extraction (QIAamp MinElute Virus Spin Kit, QIAGEN) and full length (residues 1 - 394) gD1 was cloned into mammalian expression vector (pcDNA™ 3.1 Directional TOPO® Expression Kit, Invitrogen). Full length (residues 1 - 904) glycoprotein B gene of HSV-1 strain HF (gB1) was synthesised and cloned into mammalian expression vector pcDNA3.1 (+) by Gene Synthesis Service of Genscript®. HEK 293T cells were seeded (4x10⁵/well) in 6-wells plate and the next day transfected with the gD1-expression vector or gB1-expression vector and Lipofectamine® 2000 Transfection Reagent (ThermoFisher Scientific) in Opti-MEM® Reduced Serum Medium (Gibco®, ThermoFisher Scientific). 6 h later the medium was replaced with serum-free

DMEM without antibiotics and the transgene expression was tested after 48 h. The cells were harvested and, after washing twice with Phosphate-Buffered Saline (PBS Gibco®, ThermoFisher Scientific) at 200 x g for 5 min, spun onto microscope slides by use of a cytocentrifuge at 91 x g for 3 min. The cells were then fixed with 1:1 solution of acetone/methanol and stained. In details, anti-HSV1 + HSV2 gD antibody [2C10] and anti-HSV1 + HSV2 gB antibody [10B7] were used as positive control and detected with Goat anti-Mouse IgG (H+L) Alexa Fluor 546® (A-11030, ThermoFisher Scientific). Fab#33 was used as primary antibody and Goat anti-Human IgG (H+L) Alexa Fluor® 488 (A-11013, ThermoFisher Scientific) was used for its detection. Nuclei were stained using Hoechst 33258 (Sigma-Aldrich). The images were acquired with Zeiss Axio Observer.Z1 microscope with QImaging Exi-Blue (Carl Zeiss, Oberkochen, Germany) at a 20-fold magnification.

Phenotypic assay for the evaluation of ACV susceptibility. The assay already described by Leary (Leary et al., 2002) was used following the procedure to perform PRA above described. In brief, after virus entry, different concentration of acyclovir (Acycloguanosine, ACV, Sigma-Aldrich) were used in solid agarose medium (agarose concentration 1%).

Post-attachment neutralisation assay. 100 PFU of HSV-1 HF or HSV-2 MS were added at 4°C Vero E6 cell monolayers, pre-chilled at 4°C for 15 min. After 90 min, the inoculum was removed and serial dilutions of the different antibody formats in DMEM were added at 4°C. After 90 min, medium was replaced with complete DMEM with 2% FBS and 1% Agarose (BD) and plates were incubated for 46h at 37°C. Cells were then fixed and stained (Burioni et al., 1994).

SUPPLEMENTARY FIGURES

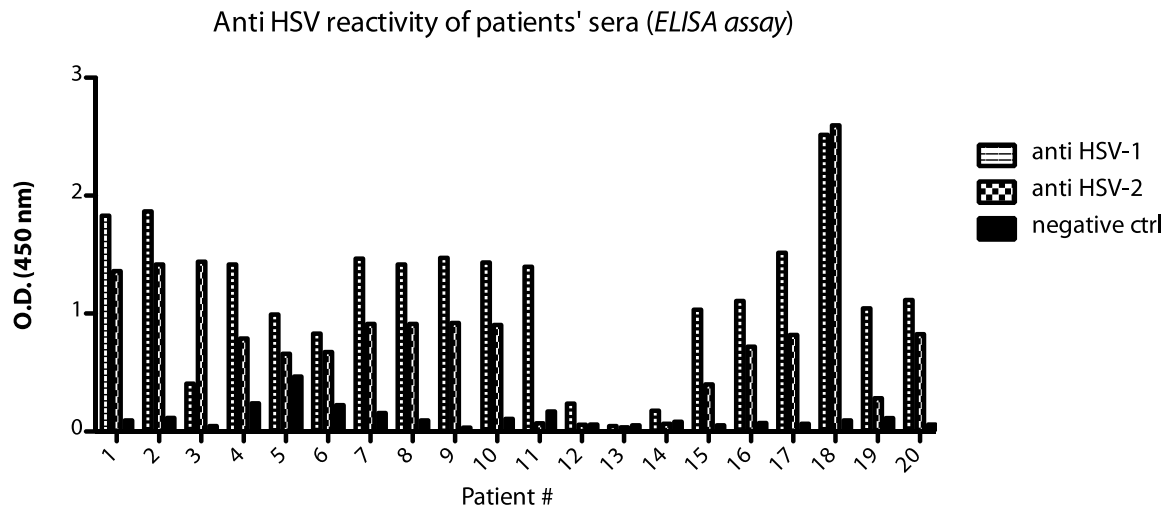
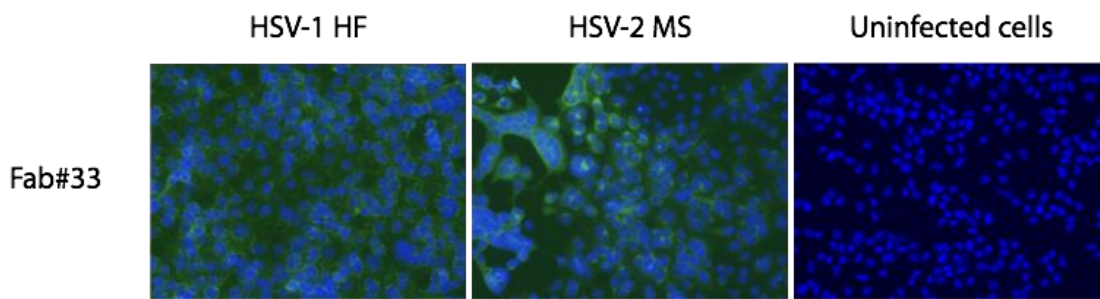


Fig. S1. ELISA assays. 20 different human sera tested against lysate HSV-1 and HSV-2 infected Vero E6 cells coated on 96-wells flat bottom microtiter plates. Patient 18 was chosen as source of peripheral blood mononuclear cells for the antibody phage display library construction.

A



B

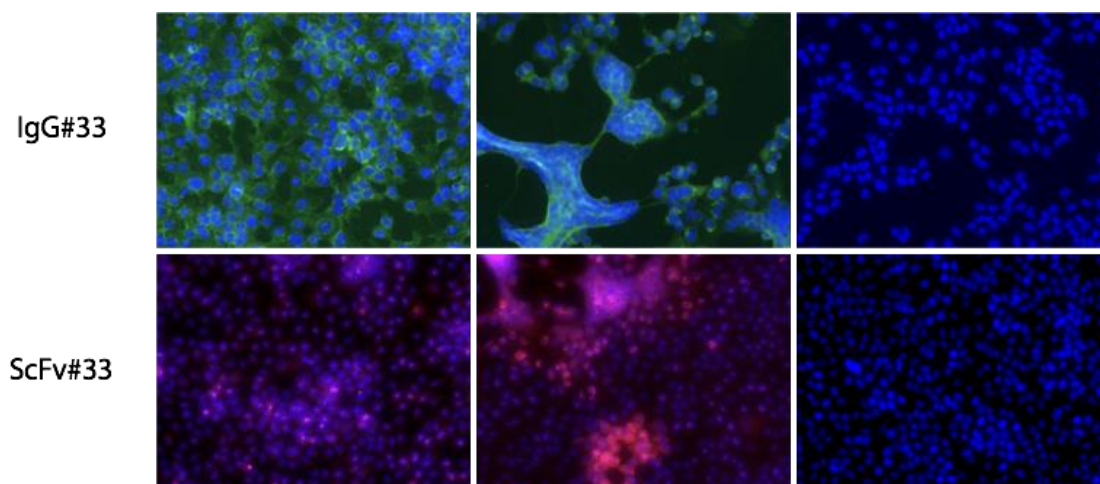


Fig. S2. Binding studies performed on HSV infected cells. (A) Vero E6 cells infected with either HSV-1 HF or HSV-2 MS ATCC strains (left to right). Blue and green signals highlight cell nuclei and Fab#33 selective binding to infected cells, respectively **(B)** Similar IIF analysis performed with IgG#33 and scFv#33 engineered molecular formats of Hu-mAb#33. Blue signal highlights cell nuclei, green and red signals indicate the specific binding to HSV-1 and 2 infected cells of IgG#33 and scFv#33, respectively. (Magnification 20x).

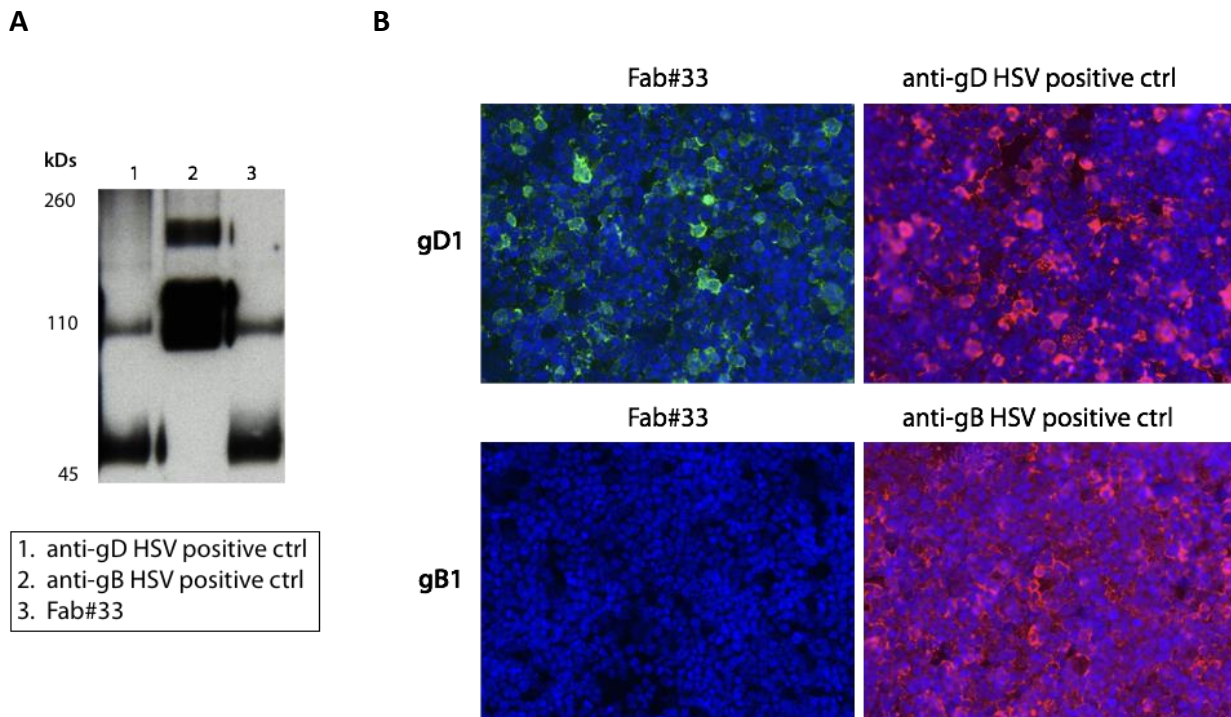


Fig. S3. Fab#33 target identification. (A) HSV-1 purified virus SDS-PAGE followed by WB analysis using Fab#33 and commercial mAb controls. The three lanes are stained as follows: (1) murine anti-HSV gD commercial control, (2) murine anti-HSV gB commercial control, (3) Fab#33. The WB reactivity pattern of Fab#33 (lane 3) is comparable with that of anti-gD monoclonal Ab (lane 1), indicating that they recognise virus protein featuring the same molecular weights. The anti-gB mAb control detects virus gB at its different molecular weights. Both gD and gB molecular weights detected in WB analysis are coherent to literature data (58 kDs monomeric gD, 116 kDs dimeric gD) (Cohen et al., 1986). **(B) IIF analysis on gD and gB expressing HEK 293T cells.** Cells transfected with gD1 (upper row) and gB1 (lower row). Green signal indicates Fab#33 selective binding to gD1 expressing cells. No green signal detected for Fab#33 on gB1 expressing cells. Red signals show selective binding of commercially available controls to gD1 and gB1 proteins. Blue signal highlights cell nuclei. (Magnification 20x).

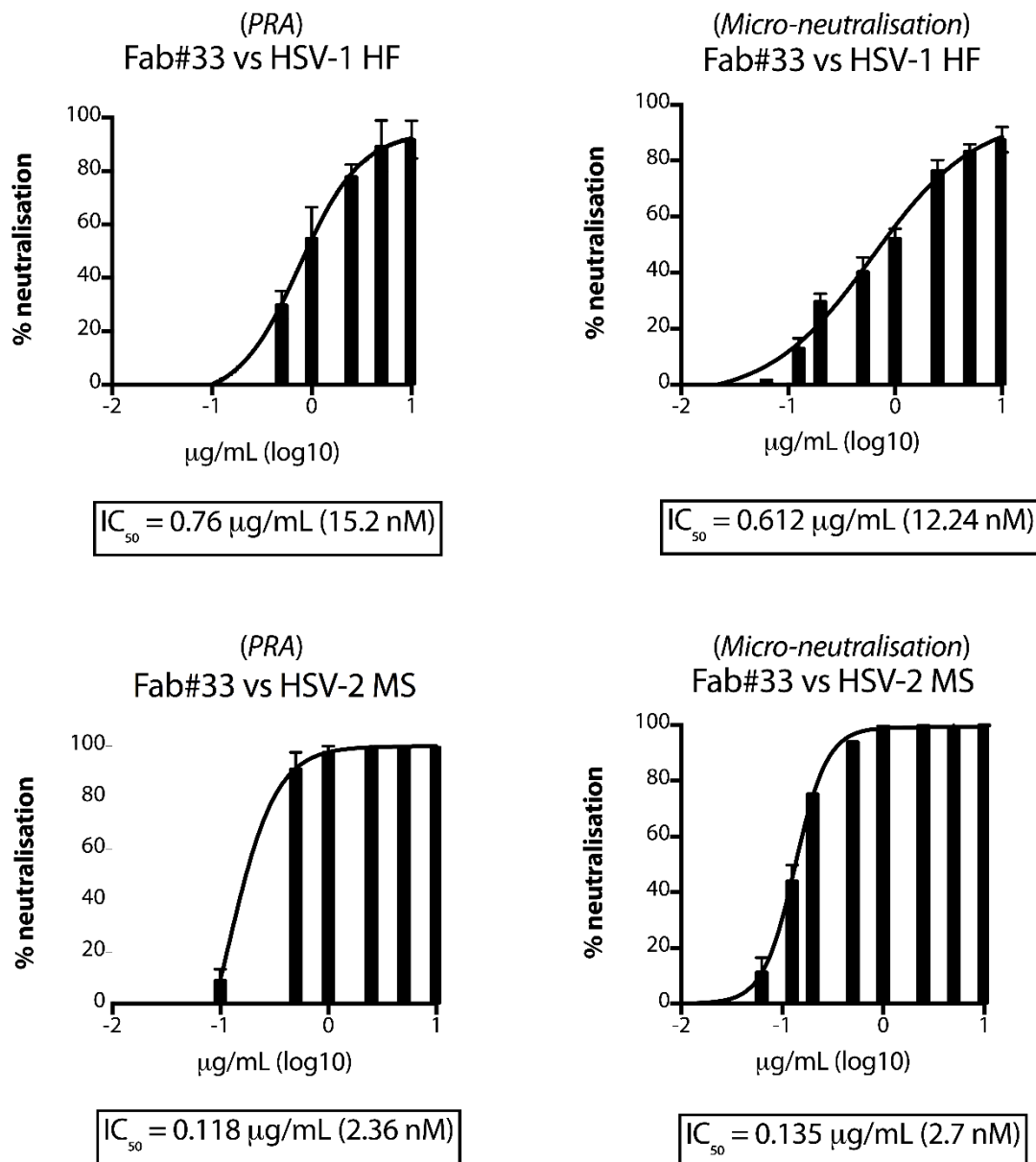


Fig. S4. Neutralisation assays performed using two techniques. Fab#33 neutralising activity evaluated against both HSV-1 and 2 laboratory strains (HF and MS respectively). Neutralisation tests were performed in triplicate using two approaches: micro-neutralisation assay followed by automated count and plaque assay. The black boxes indicate the IC_{50} calculated for Fab#33 against the two tested viruses to compare the two techniques. Percentage neutralisation was obtained by comparing the number of plaques or immunofluorescent infectious foci resulting from neutralisation mix infection (Fab#33/virus) of Vero E6 cells to number of infection events counted on cell infected with the virus alone.

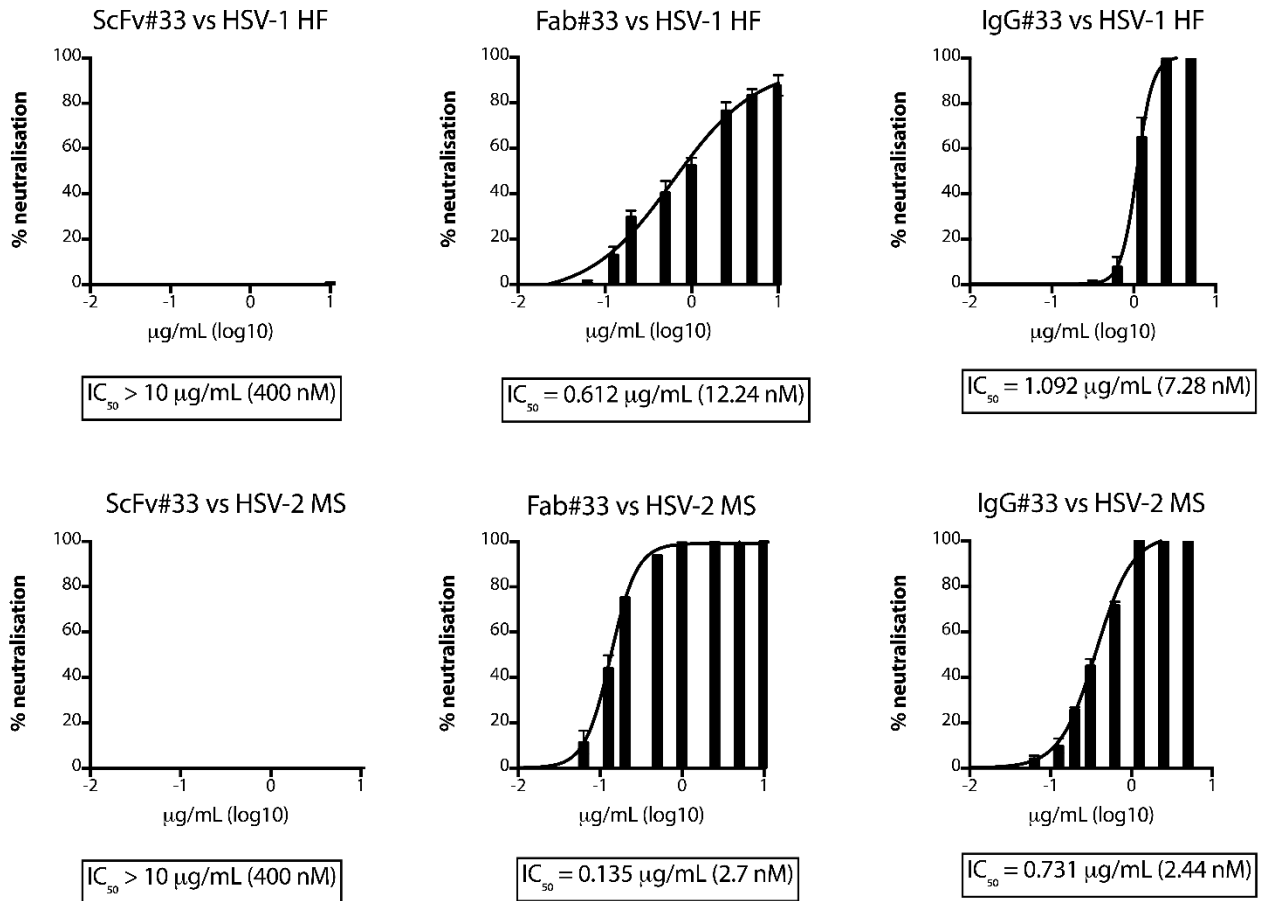


Fig. S5. Neutralising activity of different Hu-mAb#33 engineered formats. Serial dilutions of scFv#33, Fab#33 and IgG#33 were tested against two laboratory HSV isolates of type 1 and 2 (HF and MS). Micro-neutralisation assays followed by automated count analysis allowed calculation of the IC₅₀ (boxes) of the three engineered mAb formats.

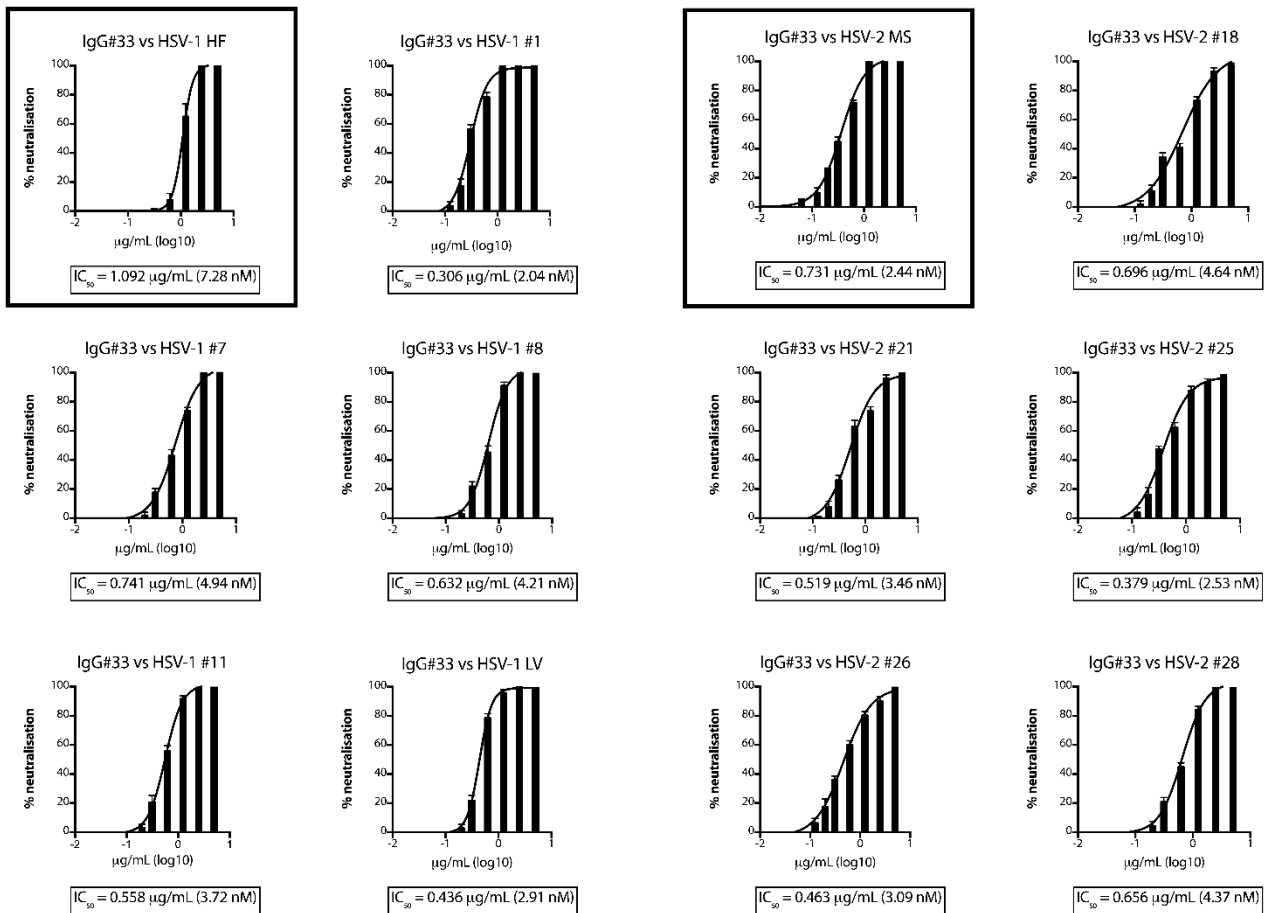
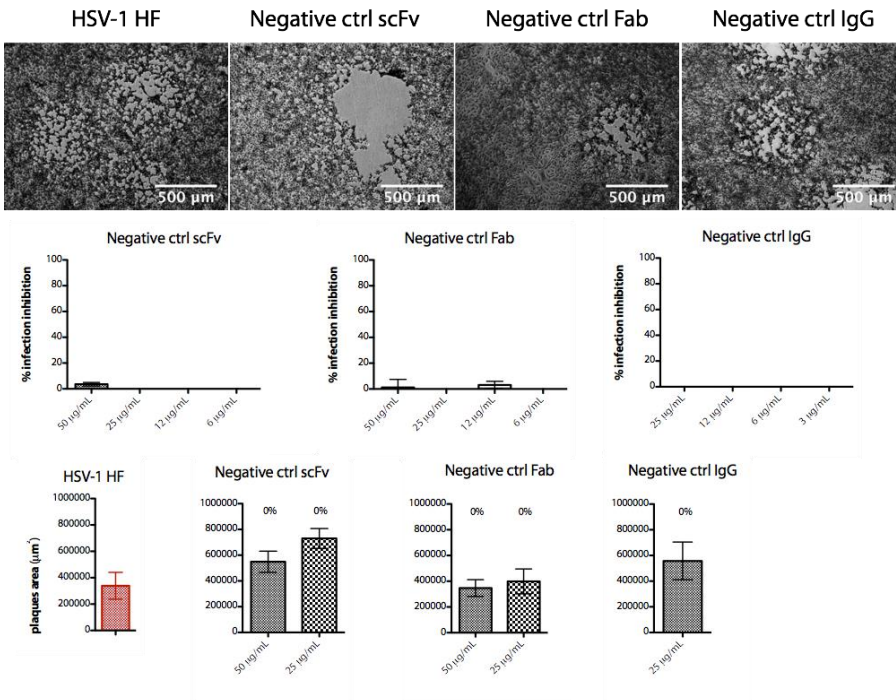


Fig. S6. Neutralising activity of IgG#33 vs HSV clinical isolates featuring different susceptibility to ACV *in vitro*. Serial IgG#33 concentrations were tested against five HSV clinical isolates of type 1 (LV, #1, #7, #8 and #11) and five of type 2 (#18, #21, #25, #26 and #28). HSV-1 and 2 laboratory strains (HF and MS) are given for comparisons (black boxes). Micro-neutralisation assay followed by automated count analysis allowed calculating IgG IC₅₀ against all the tested clinical isolates.

A



B

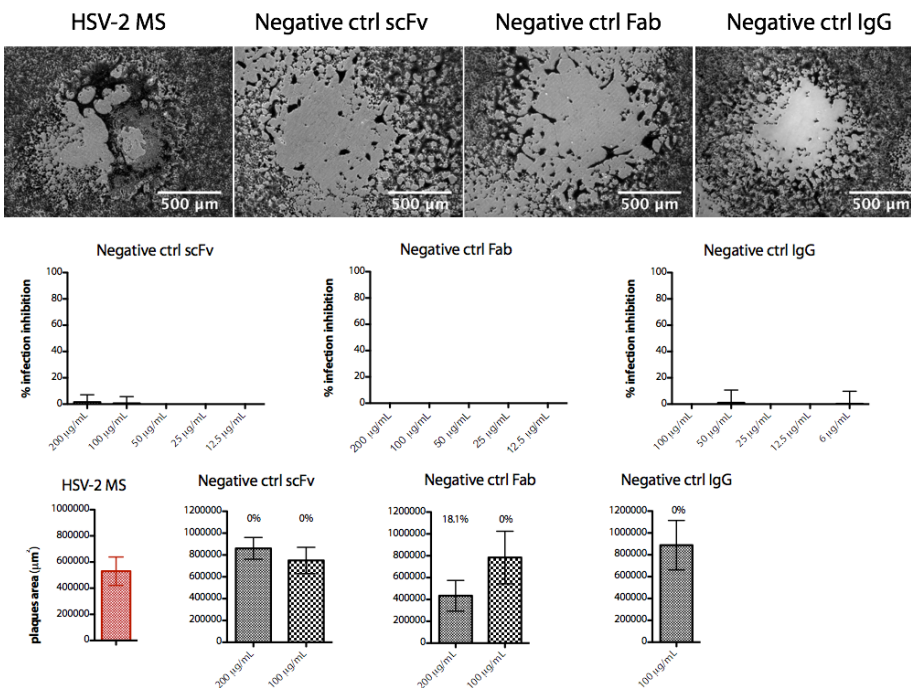


Fig. S7. Post-virus entry assays. Bright-field optical microscopy pictures collected for cells treated with the virus alone (positive infection control) and negative controls. Overview on the lack of

inhibitory activity of the experimental controls compared to HSV positive infection controls. Bar 500 μm , magnification 5x. Columns (left to right) show respectively virus positive infection controls and negative controls. Inhibition of plaque number is indicated as “% infection inhibition” on second rows. Third rows depict plaque area means (expressed in μm^2) and upper and lower 95% CI from mean (above each column, the percentages indicating plaque area reduction compared to virus control is indicated). mAb controls tested against HSV-1 HF **(A)** and HSV-2 MS **(B)**.

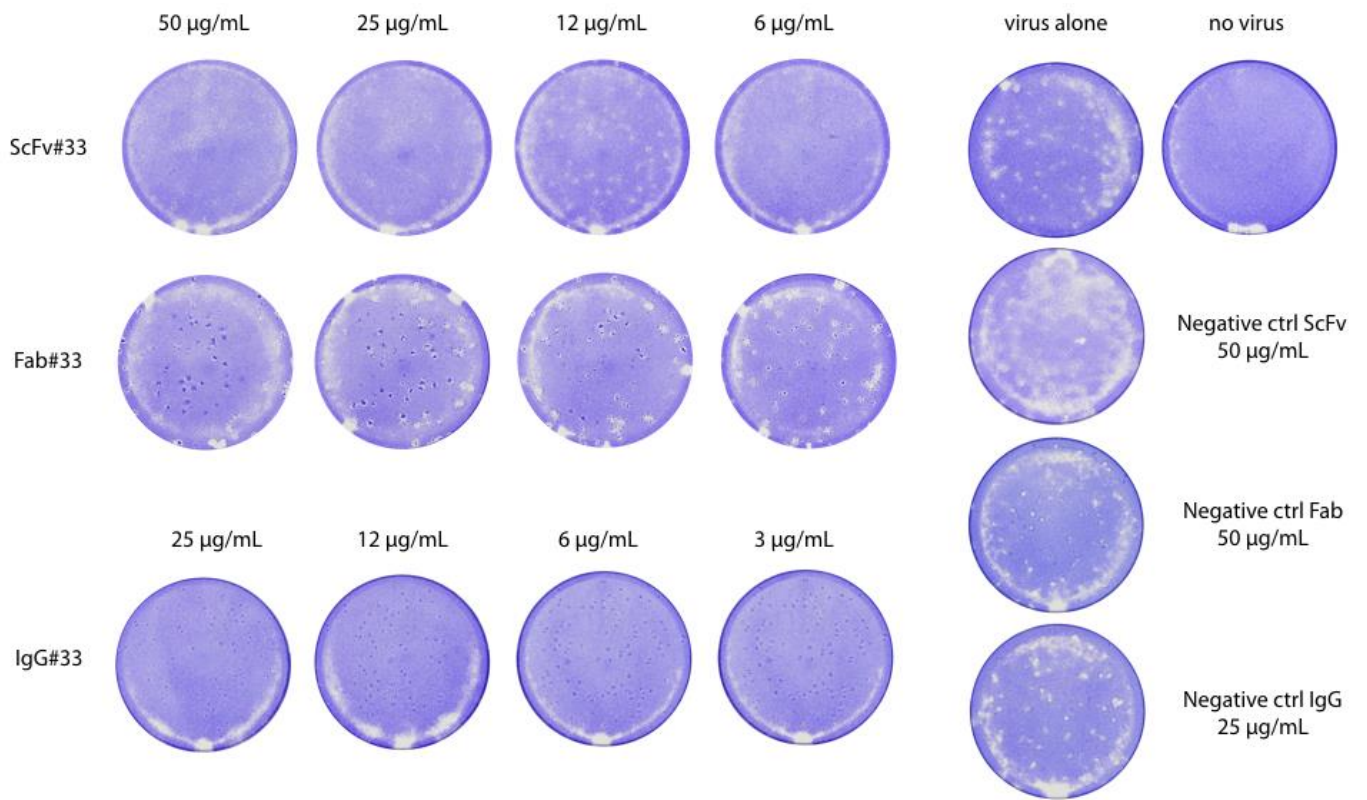
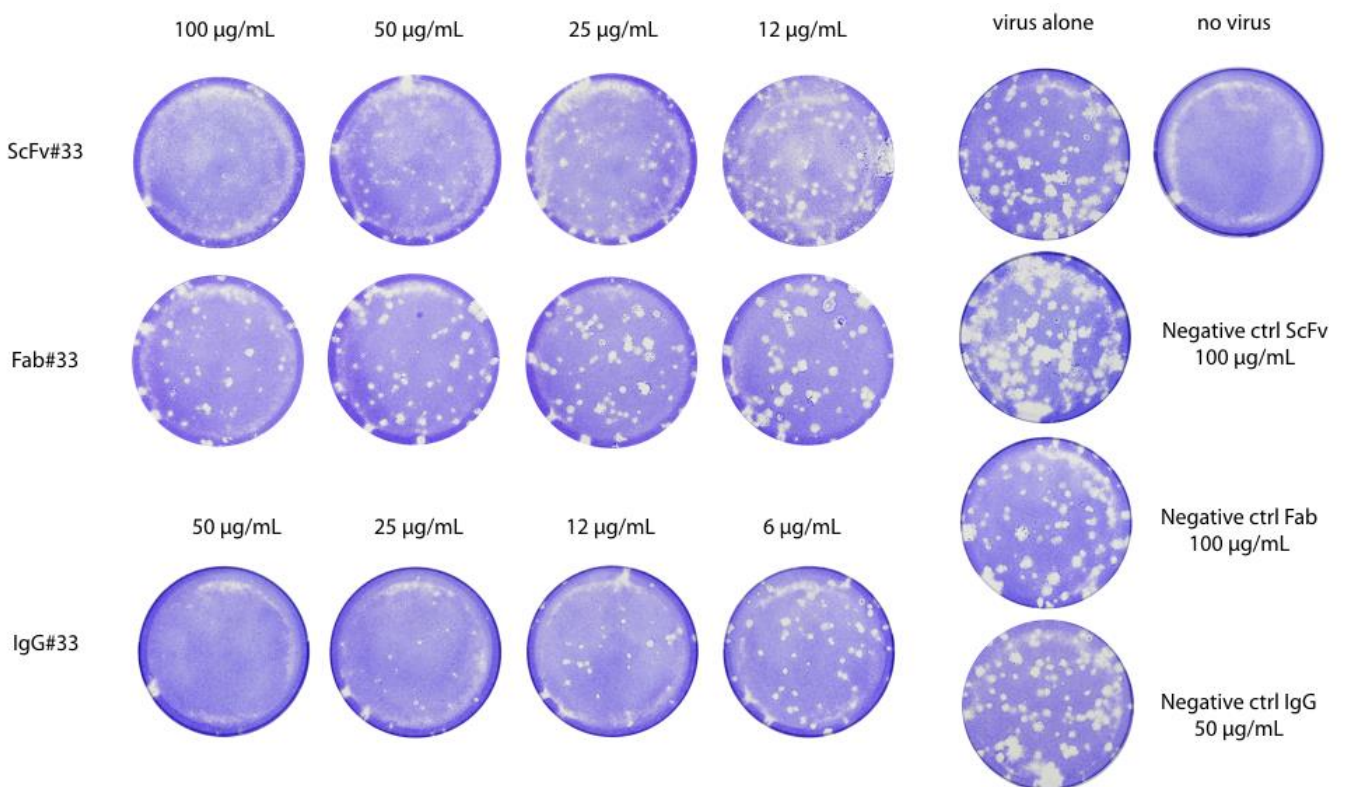
A**B**

Fig. S8. Plaque assays. scFv#33, Fab#33 and IgG#33 tested in post-virus entry assays in order to evaluate mean reduction of plaque number and areas compared to positive infection control. The three engineered mAb formats have been tested against HSV-1HF (**A**) and HSV-2 MS (**B**).

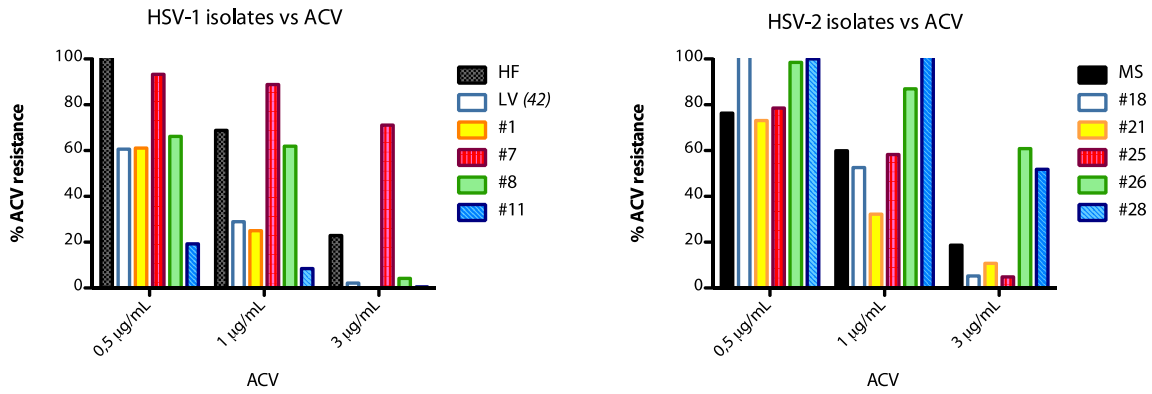


Fig. S9. Phenotypic assay on Vero E6 cells for evaluation of acyclovir susceptibility of different HSV-1 and HSV-2 clinical isolates. Susceptibility to ACV is represented on the y-axis (expressed in percentage and normalised to number of plaques of tested isolates on Vero E6 cells without ACV) of 5 clinical isolates of type 1 and 5 of type 2.

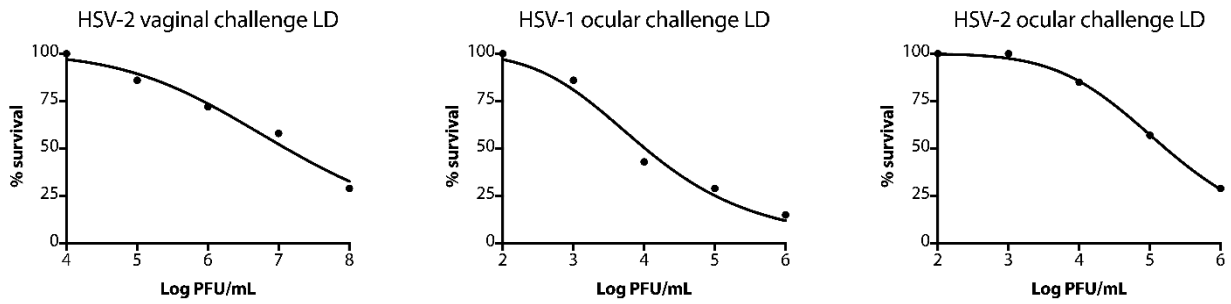


Fig. S10. LD₅₀ for HSV-1 and HSV-2 in all experimental settings. The lethal dose 50 (LD₅₀) of both HSV-1 and-2 viruses was assessed for either protocols of infection. Both virus types determine an irreversible condition at day 8 p.i. for HSV-2 MS (both for vaginal and ocular challenge) and at day 13 p.i. for HSV-1 LV ocular virus challenge.

IgG#33

Negative ctrl IgG

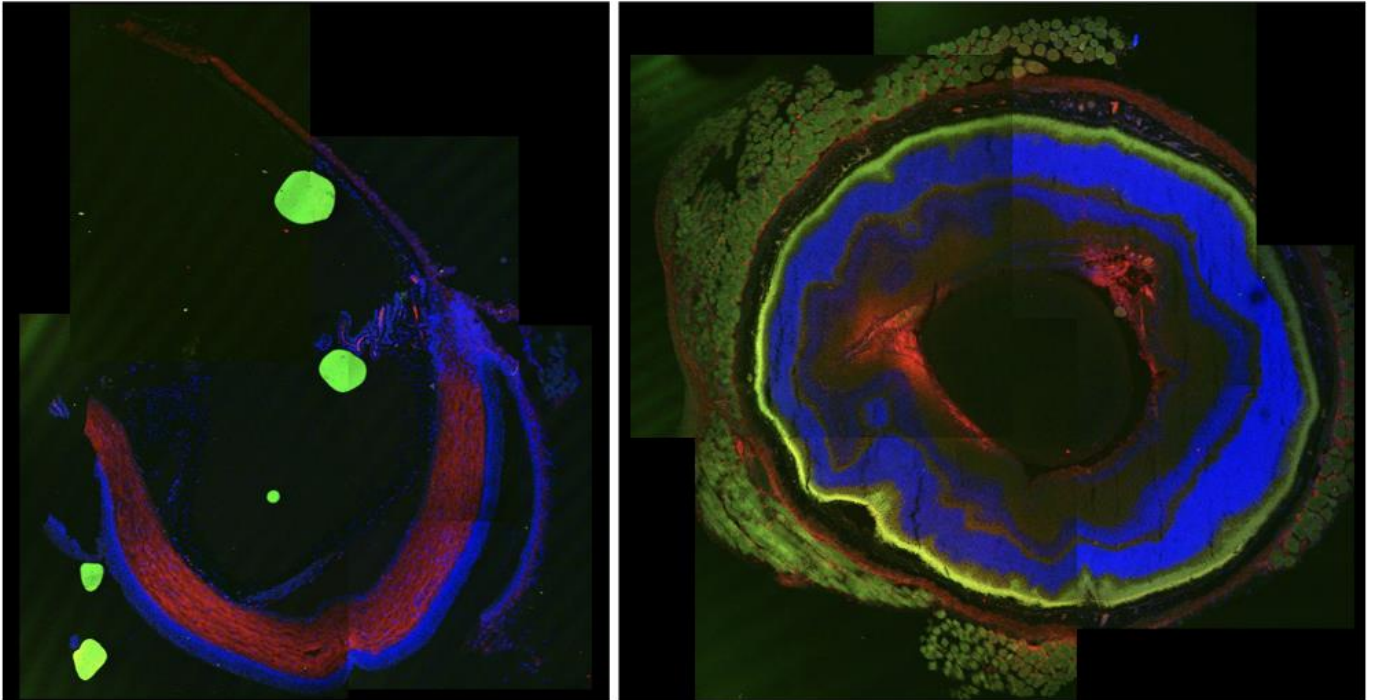


Fig. S11. Immunohistochemical analysis of HSV-2 infected mice eyes after sacrifice. 10-fold magnification pictures (merge of pictures), 1st and 2nd on the left, show an overview of the whole eye lens axis cryosection for eye of IgG#33 treated mouse receiving single systemic injection (15 mg/Kg) and Listing's plane cryosection for eye of IgG control (15 mg/Kg) treated mouse. Green fluorescence highlights F-actin bound by Phalloidin Alexa Fluor 488[®], red signal (anti-HSV1 + HSV2 gD antibody Alexa Fluor 546[®]) indicates virus presence and blue Hoechst signal indicates nuclei.

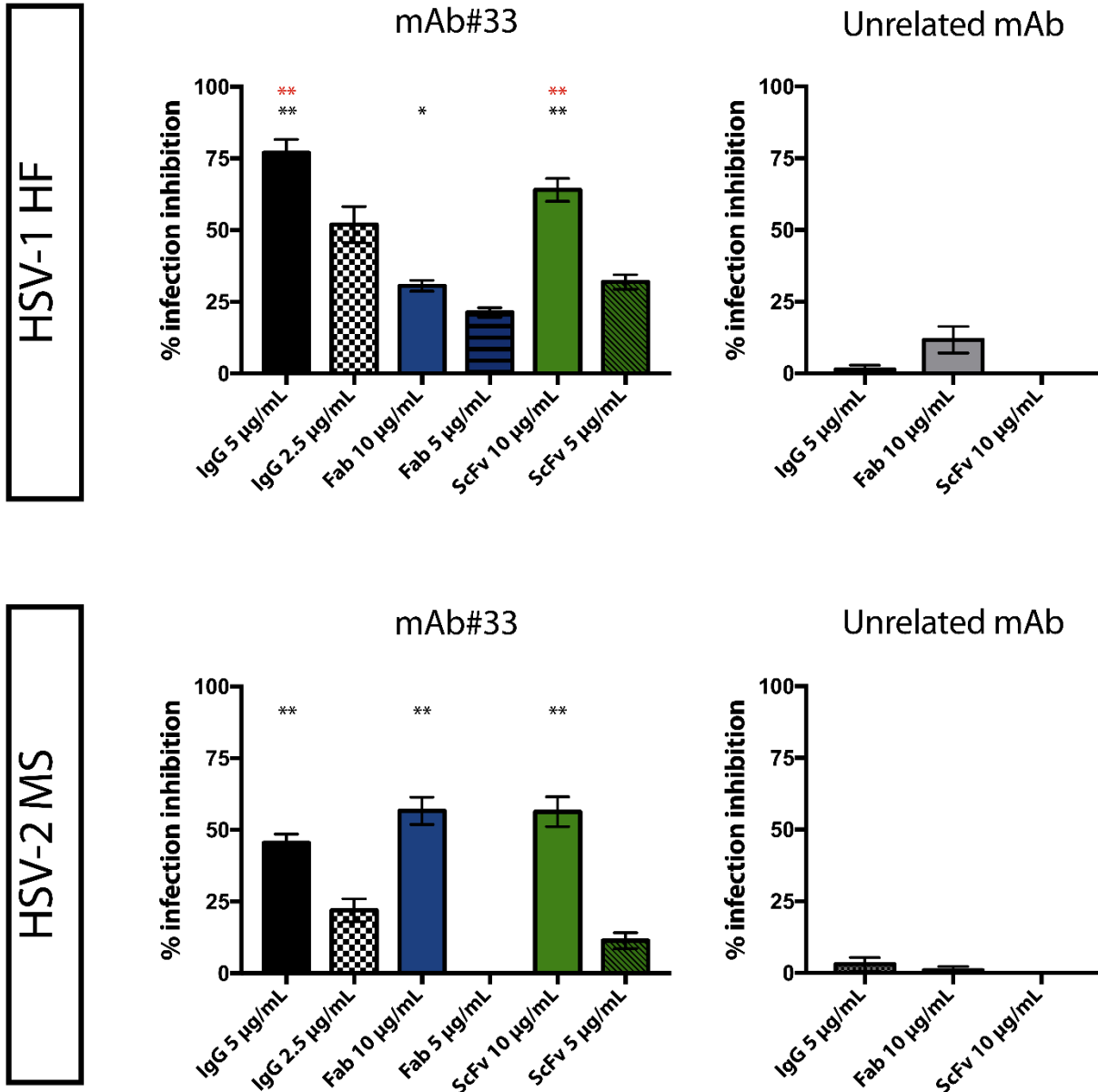


Fig. S12. Post virus attachment assay. Two concentrations of ScFv#33, Fab#33 and IgG#33 were tested against HSV-1 HF and HSV-2 MS in post virus attachment assay performed at 4°C. Statistically significant differences were observed when comparing mAb#33 to mAb mock control, (black asterisks), and Fab#33 to IgG#33 or scFv#33, (red asterisks). **p<0.01, *p<0.05.

			20			40	
HSV-1 HF (ABI63524.1)	MG	GAAARLGA	VILFVVI	VGL	HGVRGKYALA	DASLKMADPN	RFRGKDL PVL 50
HSV-2 MS (EU445527.1)	MG	RLTSGVGT	AALLVVA	VGL	RVVCAKYALA	DPSLKMADPN	RFRGKNL PVL 50
		60			80		100
HSV-1 HF (ABI63524.1)	DQL	TDP PGVR	R	VYHIQAGLP	DPFQPPSLPI	TVYYAVLERA	CRSVLLNAPS 100
HSV-2 MS (EU445527.1)	DQL	TDP PGVK	R	VYHIQPSLE	DPFQPPSLPI	TVYYAVLERA	CRSVLLHAPS 100
		120			140		
HSV-1 HF (ABI63524.1)	EAPQIVRGAS	EDVRKQPYNL	TIAWFRMGGN	CAIPITVMEY	TECSYNKSLG	150	
HSV-2 MS (EU445527.1)	EAPQIVRGAS	DEARKHTYNL	TIAWYRMGDN	CAIPITVMEY	TECPYNKSLG	150	
		160		180		200	
HSV-1 HF (ABI63524.1)	ACPIRTQPRW	NYYDSFSAVS	EDNLGFLMHA	PAFETAGTYL	RLVKINDWTE	200	
HSV-2 MS (EU445527.1)	VCPVRTQPRW	SYYSFSAVS	EDNLGFLMHA	PAFETAGTYL	RLVKINDWTE	200	
		220			240		
HSV-1 HF (ABI63524.1)	ITQFILEHRA	KGSCKYAIPL	RIPPSACLSP	QAYQQGVTVD	SIGMLPRFIP	250	
HSV-2 MS (EU445527.1)	ITQFILEHRA	RASCKYALPL	RIPPAACLTS	KAYQQGVTVD	SIGMLPRFIP	250	
		260		280		300	
HSV-1 HF (ABI63524.1)	ENQRTVAVYS	LKIAGWHGPK	APYTSTLLPP	ELSETPNATQ	PELAPEDPED	300	
HSV-2 MS (EU445527.1)	ENQRTVALYS	LKIAGWHGPK	PPYTSTLLPP	ELSDTTNATQ	PELVPEDEPED	300	
		320			340		
HSV-1 HF (ABI63524.1)	SALLEDPVGT	VAPQIPPNWH	IPSIQDAATP	YHPPATPNNM	GLIAGAVVGG	350	
HSV-2 MS (EU445527.1)	SALLEDPAGT	VSSQIPPNWH	IPSIQDVA-P	HHAPAAPSNP	GLIIGALVAG	349	
		360		380			
HSV-1 HF (ABI63524.1)	LLVALVLCGI	VYWMRRRTQK	APKRI RLP HI	REDDQPS SHQ	PLFY	394	
HSV-2 MS (EU445527.1)	TLAVLVIGGI	AFWVRRRAQM	APKRL RLP HI	RDDDAPPSHQ	PLFY	393	

Fig. S13. gD1 and gD2 amino acid sequences alignment. Alignment of HSV-1 HF glycoprotein D sequence (GenBank: ABI63524.1) and HSV-2 MS glycoprotein D (GenBank: EU445527.1).

Differences are highlighted in blue.